

1 **Oxygenated VOCs as significant but varied contributors**
2 **to VOC emissions from vehicles**

3 Sihang Wang^{1,2}, Bin Yuan^{1,2,*}, Caihong Wu^{1,2}, Chaomin Wang^{1,2}, Tiange Li^{1,2}, Xianjun
4 He^{1,2}, Yibo Huangfu^{1,2}, Jipeng Qi^{1,2}, Xiao-Bing Li^{1,2}, Qing'e Sha^{1,2}, Manni Zhu^{1,2},
5 Shengrong Lou³, Hongli Wang³, Thomas Karl⁴, Martin Graus⁴, Zibing Yuan^{5*}, Min
6 Shao^{1,2}

7 ¹ Institute for Environmental and Climate Research, Jinan University, Guangzhou
8 511443, China

9 ² Guangdong-Hongkong-Macau Joint Laboratory of Collaborative Innovation for
10 Environmental Quality, Guangzhou 511443, China

11 ³ State Environmental Protection Key Laboratory of Formation and Prevention of
12 Urban Air Pollution Complex, Shanghai Academy of Environmental Sciences,
13 Shanghai 200233, China

14 ⁴ Department of Atmospheric and Cryospheric Sciences, University of Innsbruck,
15 Innsbruck, Austria

16 ⁵ College of Environment and Energy, South China University of Technology,
17 University Town, Guangzhou 510006, China

18
19
20 *Correspondence to: Bin Yuan (byuan@jnu.edu.cn) and Zibing Yuan
21 (zibing@scut.edu.cn)

23 **Abstract:**

24 Vehicular emission is an important source for volatile organic compounds (VOCs) in
25 urban and downwind regions. In this study, we conducted a chassis dynamometer study
26 to investigate VOC emissions from vehicles using gasoline, diesel, and liquefied
27 petroleum gas (LPG) as fuel. Time-resolved VOC emissions from vehicles are
28 chemically characterized by a proton-transfer-reaction time-of-flight mass
29 spectrometry (PTR-ToF-MS) with high frequency. Our results show that emission
30 factors of VOCs generally decrease with the improvement of emission standard for
31 gasoline vehicles, whereas variations of emission factors for diesel vehicles with
32 emission standards are more diverse. Mass spectra analysis of PTR-ToF-MS suggest
33 that cold start significantly influence VOCs emission of gasoline vehicles, while the
34 influences are less important for diesel vehicles. Large differences of VOC emissions
35 between gasoline and diesel vehicles are observed with emission factors of most VOC
36 species from diesel vehicles being higher than gasoline vehicles, especially for most
37 oxygenated volatile organic compounds (OVOCs) and heavier aromatics. These results
38 indicate quantification of heavier species by PTR-ToF-MS may be important in
39 characterization of vehicular exhausts. Our results suggest that VOC pairs (e.g. C₁₄
40 aromatics/toluene ratio) could potentially provide good indicators for distinguishing
41 emissions from gasoline and diesel vehicles. The fractions of OVOCs in total VOC
42 emissions are determined by combining measurements of hydrocarbons from canisters
43 and online observations of PTR-ToF-MS. We show that OVOCs contribute $9.4\% \pm 5.6\%$
44 of total VOC emissions for gasoline vehicles, while the fractions are significantly
45 higher for diesel vehicles (52-71%), highlighting the importance to detect these OVOC
46 species in diesel emissions. Our study demonstrated that the large number of OVOC
47 species measured by PTR-ToF-MS are important in characterization of VOC emissions
48 from vehicles.

49

50 **1. Introduction**

51 Volatile organic compounds (VOCs) are important trace components in the
52 troposphere, as important precursors of ground-level ozone (Shao et al., 2009) and
53 secondary organic aerosol (SOA) (Seinfeld and Pandis, 2006;Kansal, 2009;Ziemann
54 and Atkinson, 2012). As the result, it is particularly important to identify emission
55 sources of VOCs in the atmosphere. Vehicular emission is an important source of VOCs
56 in cities around the world (Liu et al., 2008;Parrish et al., 2009), contributing
57 approximately 25% of total VOC emissions in China (Ou et al., 2015;Wu et al.,
58 2016;Sun et al., 2018). In order to control atmospheric pollution in urban and
59 surrounding regions, it is necessary to understand source profiles and emission
60 characteristics of VOCs from vehicles.

61 Emissions of VOCs from vehicles have been investigated extensively from
62 tunnel studies (Cui et al., 2018;Zhang et al., 2018;Song et al., 2020), on-road mobile
63 measurements (Li et al., 2017), and chassis dynamometer tests (Guo et al., 2011;Wang
64 et al., 2013;Yang et al., 2018). Previous studies demonstrated that fuel types of vehicles
65 strongly impact VOC emissions. Aromatics along with other hydrocarbons are known
66 as compounds with high emissions in exhausts of gasoline vehicles (Wang et al.,
67 2013;Ly et al., 2020). Some carbonyl compounds contribute significantly to emissions
68 of diesel vehicles, at fractions much higher than gasoline vehicles (Tsai et al., 2012;Qiao
69 et al., 2012;Yao et al., 2015;Mo et al., 2016). Moreover, there are still a large number
70 of unidentifiable compounds in diesel vehicles (May et al., 2014). Furthermore, VOC
71 emissions from vehicles significantly decreased in China due to stricter emission
72 standards (Liu et al., 2017;Sha et al., 2021). In order to reduce emissions of most
73 primary pollutants, more stringent emission standards and after-treatment devices have
74 been implemented. The emission standard of China VI has already been implemented
75 in July of 2019 in a few key cities in China and in July of 2021 nationwide. The emission
76 limits for various air pollutants emitted by vehicles are significantly lower under the
77 China VI emission standard (see details in the Supplement) (Wu et al., 2017). With the
78 continuous development of engine and exhaust after-treatment technologies, emission

79 characteristics of VOCs from vehicles may change and need to be frequently updated.

80 Oxygenated volatile organic compounds (OVOCs) were found to be an important
81 class of compounds in vehicle exhausts, accounting for more than 50% of the total VOC
82 emissions for diesel vehicles from both chassis dynamometer tests (Schauer et al.,
83 1999; Mo et al., 2016) and on-road mobile measurements (Yao et al., 2015).
84 Traditionally, VOCs are collected in the canister or Tedlar bags, and then analyzed by
85 gas chromatography-mass spectrometer/flame ionization detector (GC-MS/FID),
86 mainly reporting emissions of hydrocarbons (Wang et al., 2017; Qi et al., 2019).
87 Previous work usually collected 2,4-dinitrophenylhydrazine (DNPH) cartridges and
88 analyzed them using high-performance liquid chromatography (HPLC) for carbonyls
89 (aldehydes and ketones), which are both time-consuming and prone to contaminations
90 (Mo et al., 2016; Han et al., 2019).

91 The large variability of VOC emissions under different engine activities or
92 driving conditions require characterization of vehicular emissions at higher time
93 resolution. Proton-transfer-reaction mass spectrometry (PTR-MS) has been used in a
94 number of studies for measurements of vehicle emissions. VOCs from vehicle exhausts
95 under various driving and operational modes were measured by PTR-MS onboard a
96 mobile laboratory (Zavala et al., 2006; Zavala et al., 2009). Drozd et al. (2016) used a
97 PTR-MS to emphasize the importance of cold start for vehicles, concluding that VOC
98 emissions during cold start were equal to a 200 miles distance of driving during hot
99 stabilized condition. Proton-transfer-reaction time-of-flight mass spectrometry (PTR-
100 ToF-MS) can provide more powerful detection of various VOCs, thanks to the
101 measurements of whole mass spectra and high mass resolution (Cappellin et al.,
102 2012; Yuan et al., 2017). More OVOC species could be quantified from the measured
103 mass spectra based on parameterization methods for sensitivity of instrument
104 (Sekimoto et al., 2017; Wu et al., 2020).

105 In this study, we applied a PTR-ToF-MS along with a suite of other instruments
106 to measure VOCs emitted from gasoline, diesel, and liquefied petroleum gas (LPG)
107 vehicles. We investigated emission factors from different fuel types and emission
108 standards for representative VOC species exhausted from these vehicles. We used the

109 dataset to analyze contributions of various VOC groups to total VOC emissions in
110 different types of vehicles.

111 **2. Materials and methods**

112 **2.1 Tested vehicles and the chassis dynamometer study methods**

113 In this study, we conducted chassis dynamometer measurements to investigate
114 VOC emissions from vehicles using gasoline, diesel, LPG as fuel. All gasoline vehicles
115 are light-duty-gasoline-vehicle (LDGV) with the emission standards from China I to
116 China VI, whereas diesel vehicles can be classified into light-duty-diesel-truck (LDDT),
117 middle-duty-diesel-truck (MDDT), heavy-duty-diesel-truck (HDDT), and bus
118 associated with emission standards of China III to China V. In addition, the test vehicles
119 using LPG are all taxis, which are under mandatory scrappage after 8 years of driving
120 in China; as a result only China IV and China V for LPG vehicles were tested. After-
121 treatment devices commonly used in light-duty gasoline vehicles are three-way catalyst
122 (TWC) and gasoline particulate filter (GPF) (Lyu et al., 2020). These devices have been
123 improved with the stricter emission standards. For diesel vehicles, typical after-
124 treatment devices include diesel oxidation catalyst (DOC), diesel particulate filter
125 (DPF), and selective catalyst reduction (SCR) (Zhou et al., 2019;Lyu et al., 2020;Shen
126 et al., 2021). The diesel vehicles for China III or prior do not have any after-treatment
127 devices. Light-duty-diesel-truck (LDDT) used DOC and DOC+DPF as after-treatment
128 devices in China IV and V diesel vehicles, respectively. SCR devices are mainly used
129 for heavy-duty-diesel-truck (HDDT) with China IV and V as after-treatment devices.
130 The fractions of gasoline and diesel vehicles with different emission standards in China
131 are shown in Table S1 (MEEPRC, 2019;Li et al., 2021). Among the 38 vehicles we
132 tested, a fraction of vehicles was measured several times, with a total of 62 experiments
133 measured. The detailed information for test vehicles is summarized in Sect. 1 in the
134 Supplement, Table S2 and Table S3.

135 The short transient driving cycle (GB 18285-2018, Figure S1a), as one of the
136 widely used test methods for vehicle emissions in China (Li et al., 2012;Wang et al.,
137 2013), was used for measurements of gasoline vehicles and LDDT, each running for

138 three to five times. The short transient driving cycle methods were initially adapted
139 based on emission regulations of the Economic Commission for Europe (ECE) cycle
140 (Yao et al., 2003), which is developed and used in European countries (Laurikko, 1995).
141 The short transient driving cycle consist of four conditions, namely idling, acceleration,
142 deceleration and uniform speed, as shown in Fig. S1. For the MDDT and HDDT, we
143 customized a step-by-step test method, in which the vehicle accelerates to 20 km·h⁻¹,
144 40 km·h⁻¹ and 60 km·h⁻¹ in sequence after the engine activates, keeping at 20 km·h⁻¹
145 and 40 km·h⁻¹ for 2 minutes, and 60 km·h⁻¹ for 1 minute, respectively (Fig. S1) (Li et
146 al., 2021;Liu et al., 2021;Liao et al., 2021). In addition, the cold start was tested for a
147 number of vehicles after a cold soak for more than 12 hours at ambient temperature
148 (20-25 °C) before engine started. The measurements of cold start are compared to
149 measurements of hot start after a ~10 minutes break for the vehicles after previous
150 measurement. More details about cold start and hot start in this campaign can be found
151 in Li et al. (2021).

152 A custom-built sampling and dilution system for vehicles combining online and
153 offline sampling techniques was used in this study. As shown in Fig. S2, a portable
154 emission measurement system (PEMS, SEMTECH-DS, Sensors. USA) was employed
155 to measure emissions of CO, CO₂, NO_x, and total hydrocarbon (THC) directly from the
156 tailpipe of vehicles. A custom-built dilution system (Li et al., 2021;Liao et al., 2021)
157 was used for dilution of vehicular emissions, achieving dilution ratios of 10-100 for
158 different vehicles. After dilution, CO₂ and CO were measured using a Li-840A
159 CO₂/H₂O Gas Analyzer (Licor, Inc. USA) and a Thermo 48i-TLE analyzer (Thermo
160 Fisher Scientific Inc. USA), respectively. Measurements of CO₂ before and after the
161 dilution system was used to determine the dilution ratio for each test (see details in Fig.
162 S3).

163 **2.2 VOC measurements using PTR-ToF-MS**

164 In this study, a Proton Transfer Reaction Quadrupole interface Time-of-Flight
165 Mass Spectrometer (PTR-QiToF-MS) (Ionicon Analytik, Innsbruck, Austria) with
166 H₃O⁺ chemistry was used to measure VOCs (Sulzer et al., 2014). The mass spectra of

167 PTR-ToF-MS was recorded every 1 s to capture characteristics of VOC species from
168 vehicle exhausts in real-time. Background measurements of the instrument were
169 performed using sampled air through a custom-built platinum catalytical converter
170 heated to 365 °C for 30 s before vehicle starts in each test. The more detailed setting
171 parameters for the instrument can be found elsewhere (Wu et al., 2020;Wang et al.,
172 2020a;He et al., 2022). Data analysis of PTR-ToF-MS was performed using the Tofware
173 software package (version 3.0.3, Tofwerk AG, Switzerland) (Stark et al., 2015).

174 A 23-component gas standard (Linde Spectra) was used for daily calibration of
175 PTR-ToF-MS during the campaign. VOC sensitivities from automatical calibrations
176 indicated quite stable instrumental performance for most of the VOC species (Fig. S4).
177 Another gas standard with 35-component VOCs (Apel Riemer Environmental Inc.) was
178 used for calibrations during the later period of this campaign to include more VOC
179 species in the calibration. The Liquid Calibration Unit (LCU, Ionicon Analytik,
180 Innsbruck, Austria) was used to calibrate a total of 11 organic acids and nitrogen-
181 containing species (Table S4). The limits of detection for calibrated VOC species are
182 below 100 ppt for the 1-s measurement, except for ethanol (423 ppt) and formic acid
183 (166 ppt). Additionally, the humidity dependence for a few VOC species in PTR-ToF-
184 MS (Yuan et al., 2017;Koss et al., 2018) were corrected using humidity-dependence
185 curves determined in the laboratory, as previously shown in Wu et al. (2020). To
186 quantify the ion signals without calibration, we determine the sensitivities based on the
187 kinetics of proton-transfer reactions of H_3O^+ with VOCs (Cappellin et al.,
188 2012;Sekimoto et al., 2017). The relationship between VOCs sensitivity and kinetic
189 rate constants for the same instrument has been reported in Wu et al. (2020) and He et
190 al. (2022). The corrected sensitivities as a function of kinetic rate constants for proton-
191 transfer reactions of H_3O^+ with VOCs during this campaign is shown in Fig. S5. The
192 fitted line is used to determine sensitivities of uncalibrated species, and the uncertainty
193 of the concentrations for uncalibrated species are determined to be around 50%.

194 **2.3 Other VOC measurements**

195 Whole air samples were collected using canisters after the dilution system for

196 determination of hydrocarbons emitted from various vehicles. All the canisters were
197 sent to the laboratory for analysis by an offline GC-MS/FID system, with a total 95
198 hydrocarbons calibrated by Photochemical Assessment Monitoring Stations (PAMS)
199 and TO-15 standard mixtures (Table S5). We compared emission factors from PTR-
200 ToF-MS and the offline canister-GC-MS/FID (Fig. S6c-d), obtaining generally
201 consistent results, considering the large variation of VOC emissions for driving
202 conditions and the difficulty to control the fill time for canisters.

203 An instrument based on Hantzsch reaction-absorption method was used to
204 measure formaldehyde (Zhu et al., 2020). Good agreement for formaldehyde between
205 PTR-ToF-MS and the Hantzsch instrument was obtained (Fig. S6a). An iodide-adduct
206 time-of-flight chemical ionization mass spectrometer (I⁻ ToF-CIMS, Aerodyne
207 Research, Inc.) (Wang et al., 2020c; Ye et al., 2021) was used to measure organic acids,
208 hydrogen cyanide (HCN), and isocyanic acid (HNCO) from vehicles (Li et al., 2021).
209 As shown in Fig. S6b, formic acid measured by PTR-ToF-MS and I⁻ ToF-CIMS showed
210 reasonable agreement.

211 **2.4 Emission factors and emission ratios calculation**

212 In this study, we determine emission factors of VOC species in two different
213 approaches: the mileage-based emission factors ($\text{mg}\cdot\text{km}^{-1}$) as the mass of these VOCs
214 exhausted per kilometer driving of vehicles, and the fuel-based emission factors
215 ($\text{mg}\cdot\text{kg}_{\text{fuel}}^{-1}$) as the mass of VOCs per kilogram of fuel burned by the vehicles. In
216 addition, emission ratios of VOCs to combustion tracers (usually CO) are widely
217 applied in vehicle emissions in urban regions, as the result we determine emission
218 ratios to CO in $\text{ppb}\cdot\text{ppm}^{-1}$ as well. More details about the determination of emission
219 factors and emission ratios can be found in Sect. 2 in the Supplement.

220 The average emission factors for various types of vehicles are determined from
221 arithmetic means for different emission standards of vehicles. As for diesel vehicles,
222 the average emission factors are obtained from the arithmetic means of LDDT, MDDT,
223 HDDT, and bus. Besides, we also calculate emission factors and emission ratios from
224 weighted means based on the fractions of gasoline and diesel vehicles with different

225 emission standards in China (MEEPRC, 2019;Li et al., 2021) (see Sect. 2 in the
226 Supplement for details). In order to evaluate the uncertainties of obtained emission
227 factors, the average limit of detection for VOC species are used to estimate the limit
228 of detection for the determined emission factors (more details can be found in Sect. 3
229 in the Supplement).

230 **3. Results and discussions**

231 **3.1 Characteristics of the VOC emissions in the vehicles**

232 Time series of several aromatics and OVOC species measured by PTR-ToF-MS
233 for a selected gasoline vehicle associated with emission standard of China I and a LDDT
234 associated with China IV emission standard are shown in Fig. 1. Both tests started with
235 cold engines of the two vehicles. Benzene and toluene are typical aromatic species
236 emitted by vehicles. As shown in Fig. 1a, high concentrations of benzene and toluene
237 exhausted by the gasoline vehicle were observed as the engine started. The
238 concentrations of the two species continued to increase until ~2 min after the engine
239 started, and then dropped rapidly before a minor increase during the acceleration
240 condition. These observations are similar to the previous results from PTR-MS
241 measurements in Drozd et al. (2016). Acetaldehyde and acetone are important OVOC
242 species emitted from vehicles. They show similar temporal variations as benzene and
243 toluene. However, concentrations of acetaldehyde and acetone were much lower than
244 the two aromatics after engine started. Compared to the concentrations at engine start-
245 up for the gasoline vehicle (the first cycle), concentrations of the VOCs are 3.0 to 40
246 times lower during the gasoline vehicle running at hot stabilized condition (the third
247 cycle). As shown in Fig. 1 for the diesel vehicle, enhanced emissions from cold start
248 are minor, which is different from the gasoline vehicle. The concentration of these
249 VOCs at engine start-up for the diesel vehicle are only 1.3 to 2.5 times higher than the
250 periods as the diesel vehicle running at hot stabilized condition. It indicates that the
251 impact of the engine start-up on emissions in diesel vehicles is much lower than
252 gasoline vehicles. This may be explained by a combined effect of cold engine and
253 operation temperature of the after-treatment device (Gentner et al., 2017;George et al.,

254 2015). In contrast to the gasoline vehicle, we observe higher concentrations of the two
255 OVOC species than the two aromatics species, namely benzene and toluene, from the
256 diesel vehicle. These higher OVOC concentrations in diesel vehicle exhausts are in line
257 with the higher observations of organic acids using the I- ToF-CIMS from the same
258 campaign (Li et al., 2021).

259 Based on the high time-resolution measurements of PTR-ToF-MS, we
260 determined emission factors of various VOC species from different vehicles. Fig. 2
261 shows the determined average mileage-based emission factors of benzene, toluene,
262 acetaldehyde, and acetone for various types of vehicles (also tabulated in the
263 Supplement table). In general, we observe a downward trend for emissions factors of
264 gasoline vehicles from China I to China VI emission standards for the four
265 representative VOC species. This is consistent with the results in previous studies with
266 lower emissions for newer emission standards (Wang et al., 2017;Sha et al., 2021). In
267 addition, the dependence of VOCs emission versus emission standard may also be
268 attributed to the history of vehicle usage, i.e., the mileage traveled by the vehicles, as
269 lower mileages of vehicles are usually associated with vehicles with newer emission
270 standards. As shown in Fig. 3, we observe strong positive relationship between toluene
271 emission factors and vehicle odometers for both gasoline and diesel vehicles, indicating
272 the mileages of vehicles can significantly affect VOCs emission factors for vehicles
273 tested in this study. The emission factors of the representative VOC species are highest
274 for China II gasoline vehicles rather than China I vehicles, which can be explained by
275 the China II vehicles having the highest mileage of the test vehicles. Emission factors
276 of the four species for China VI vehicles are 12 to 25 times lower than emission factors
277 for China I vehicles, indicating that newer emission standards successfully reduced
278 VOC emissions of gasoline vehicles. The decline of emission factors for the four
279 species with newer emission standards for diesel vehicles are in the range of 1.1 to 7.4
280 times from China III to China V, compared to 4.5 to 5.4 times reduction from China III
281 to China V for gasoline vehicles. Emission factors of benzene and toluene from diesel
282 vehicles are in the range of 0.8 to 7.4 $\text{mg}\cdot\text{km}^{-1}$ and 0.3 to 5.8 $\text{mg}\cdot\text{km}^{-1}$, which are
283 comparable to emission factors from gasoline vehicles with China IV to China VI

284 emission standards. This is different from observations of the two OVOC species
285 (acetaldehyde and acetone), with much higher emission factors from diesel vehicles
286 (8.0 to $27.9 \text{ mg}\cdot\text{km}^{-1}$ for acetaldehyde and 0.8 to $10.0 \text{ mg}\cdot\text{km}^{-1}$ for acetone) than almost
287 all gasoline vehicles (a maximum of $3.9 \text{ mg}\cdot\text{km}^{-1}$ for acetaldehyde and a maximum of
288 $3.2 \text{ mg}\cdot\text{km}^{-1}$ for acetone). Higher emission factors from diesel vehicles are also
289 observed for many other common OVOC species, as shown in Fig. 4. As the largest
290 OVOCs emitted from gasoline vehicles ($4.6 \pm 5.1 \text{ mg}\cdot\text{km}^{-1}$), methanol is found to be
291 the only common OVOC species with lower emission factors from diesel vehicles than
292 gasoline vehicles. The emission factor of other OVOCs (e.g. formaldehyde, acetone)
293 from diesel vehicles are higher than gasoline vehicles, which is consistent with previous
294 results (Gentner et al., 2013). The high emissions of OVOCs from diesel vehicles may
295 be related to combustion processes in diesel vehicles, with more excess air present in
296 the combustion cylinder (i.e., overall fuel-lean conditions) resulting in higher oxygen
297 contents and more oxidation processes during fuel combustion (Pang et al., 2008; Qiao
298 et al., 2012; Gentner et al., 2017). Finally, the determined emission factors of the four
299 VOC species from LPG vehicles are much lower than both gasoline and diesel vehicles.

300 **3.2 Analysis of PTR-ToF-MS mass spectra to evaluate VOCs** 301 **speciation**

302 In addition to typical VOC species shown above, PTR-ToF-MS detected
303 abundant signals for a large number of ions. The determined average mileage-based
304 emission factors for all detected VOC species are shown as mass spectra in Fig. 4. VOC
305 species measured by PTR-ToF-MS were divided into groups according to chemical
306 formula, namely hydrocarbon species only containing C and H atoms (C_xH_y), OVOCs
307 ($\text{C}_x\text{H}_y\text{O}_z$), species containing nitrogen and/or sulfur atoms (N/S-containing), and some
308 other ions (others). We observe similar mass spectra of emission factors for gasoline
309 vehicles with different emission standards (Fig. S7). Highest emission factors from
310 gasoline vehicles (Fig. 5a) are detected as hydrocarbons, including C_6 to C_{10} aromatics.
311 A few OVOC species, namely methanol, ethanol, formaldehyde, acetaldehyde and
312 acetone, are also observed as the largest emissions. In contrast to gasoline vehicles, the

313 largest emissions from diesel vehicles were attributed to a few low-molecular-weight
314 OVOC species, including formaldehyde, acetaldehyde, formic acid, and acetic acid,
315 followed by a large number of hydrocarbon species. Comparison between the mass
316 spectra of gasoline and diesel vehicle emissions suggest that emissions from diesel
317 vehicles are more evenly distributed among different VOC species, as reflected by 50
318 and 140 species contributing more than 1% of the total emissions for gasoline and diesel
319 vehicles, respectively. As shown in Fig. 5b, many hydrocarbon ions in the range of m/z
320 150-200 still account for significant fractions of emissions from diesel vehicles,
321 whereas only one species in this m/z range contribute more than 1% of emissions from
322 gasoline vehicles. These results demonstrate that diesel vehicles emit more heavier
323 hydrocarbons than those from gasoline vehicles, which is consistent with observations
324 in previous studies (Gentner et al., 2012; Erickson et al., 2014).

325 The scatterplot of carbon oxidation states (\overline{OS}_C) as a function of carbon number
326 (n_C) provides a framework for describing bulk chemical properties of organics (Kroll
327 et al., 2011). The details of \overline{OS}_C calculation is included in Sect. 4 in the Supplement.
328 The results from gasoline and diesel vehicles are compared in Fig. 6 (LPG vehicles are
329 shown in Fig. S8). It is apparent that ions with carbon oxidation states between -2.0 to
330 0 comprise main emissions for each carbon number for both gasoline and diesel
331 vehicles. It is interesting to observe that averaged \overline{OS}_C for $n_C > 6$ increase as the carbon
332 number decrease for both gasoline and diesel vehicles, whereas the opposite trends are
333 observed for $n_C < 5$. The averaged \overline{OS}_C in diesel vehicles for n_C between 1 and 5 are
334 significantly higher than those in gasoline vehicles, as the result of high emissions of
335 C₂ to C₅ low-molecular-weight OVOCs. Fig. 6c further shows that emission factors of
336 most VOC species from diesel vehicles were higher than gasoline vehicles, except for
337 a number of species occupying the right-bottom corner of the two-dimensional space.

338 The determined mass spectra of PTR-ToF-MS in terms of emission factor for
339 different types of vehicles can be used to explore the dependence of various VOC
340 emissions to different factors. Fig. 7a-b shows scatterplots of the average mileage-
341 based emission factors of VOCs between cold start and hot start for gasoline and diesel
342 vehicles, respectively. We observe strong correlation between emission factors from

343 cold start and hot start tests ($R=0.99$ and 0.92) and generally consistent ratios between
344 cold start and hot start for different types of VOC species for both gasoline and diesel
345 vehicles, indicating that variation behaviors are similar for different species and thus
346 chemical compositions of VOC emissions are comparable between different start
347 conditions. As cold start emissions are richer in unburned fuel than other hot-running
348 conditions (Gentner et al., 2017) and the after-treatment devices aim for VOCs control
349 for gasoline vehicles, the strong correlation and significantly lower than unity slope in
350 Fig. 7a suggest that unburned fuel are the major contributor for exhaust emissions of
351 gasoline vehicles, which has been previously shown in California, U.S. (Gentner et al.,
352 2013). It is obvious that emission factors of VOCs during cold start are significantly
353 higher than those during hot start for gasoline vehicles (slope= 0.40), whereas similar
354 emissions factors between cold start and hot start are derived for diesel vehicles
355 (slope= 0.84). These results suggest that gasoline vehicles are more significantly
356 influenced by cold start, as the result of compositions in gasoline fuel being more
357 volatile than diesel fuel (US NRC, 1996). We further explore the effects of emission
358 standards on VOC emission factors by comparing determined emission factors
359 between China I and China V for gasoline vehicle (Fig. 7c, also see China III versus
360 China V and China V versus China VI in Fig. S9) and between China III and China V
361 for LDDT (Fig. 7d, also see China III versus China V for MDDT and HDDT in Fig.
362 S9). Fig. 7c show that the chemical compositions of VOC emissions are comparable
363 between different emission standards for abundant VOC species from gasoline
364 vehicles, indicating after-treatment devices may not affect the relative fractions of
365 VOC components for gasoline vehicles (Drozd et al., 2019; Lu et al., 2018; Zhao et al.,
366 2017). In comparison, the results between different emission standards for diesel
367 vehicles (Fig. 7d) are somewhat more scattered than in gasoline vehicles. Furthermore,
368 comparison of both gasoline and diesel vehicles demonstrate newer emission
369 standards successfully decreased VOC emissions. Based on the derived slopes, we
370 obtain VOCs emission factors that are reduced by a factor of 10 for gasoline vehicles
371 from China I to China V (a factor of 5 reduction from China III to China V and a factor
372 of 2.5 reduction for China V to China VI), and a factor of 2 for LDDT from China III

373 to China V (a factor of 1.5 and 8 reduction for MDDT and HDDT from China III to
374 China V). The reduction ratio for gasoline vehicles from China I to China V are
375 generally similar for most VOC species, except that some OVOC species showed
376 smaller reduction ratios. The reduction ratios for LDDT vehicles from China III to
377 China V show large variability for different species. The lowest reduction ratios (a
378 factor of ~2) are observed for the low-molecular weight OVOC species associated
379 with largest emissions, while the reduction ratios for hydrocarbons and higher-
380 molecular weight OVOCs are in the range of a factor of 10-100. These results indicate
381 the after-treatment device for diesel vehicles (see Sect. 1 in the Supplement for details.)
382 may effectively reduce emissions of some heavier VOC species, though the after-
383 treatment devices do not aim for VOCs control (Gentner et al., 2017).

384 **3.3 Non-target analysis for comparison between gasoline and diesel** 385 **vehicles**

386 As shown in the previous section, the analysis of PTR-ToF-MS mass spectra
387 provide rich information on understanding the influences of VOC emissions from
388 vehicles. This detailed information provided by the PTR-ToF-MS also offer an
389 opportunity to systematically compare emissions between gasoline and diesel vehicles.
390 The scatterplot of the determined average emission factors of various VOC species
391 between gasoline and diesel vehicles is shown in Fig. 8. Large differences in VOC
392 compositions emitted from gasoline and diesel vehicles are observed, as indicated by
393 the low correlation of the data points ($R=0.24$). A limited number of VOC species,
394 including C₆-C₁₀ aromatics and some N/S-containing species (e.g. C₇H₅N) are
395 associated with higher emission factors from gasoline vehicles, whereas the obtained
396 emission factors of most VOC species emitted from diesel vehicles are higher,
397 especially for most OVOC species. For example, formic acid is found to be one of the
398 most significant species emitted by diesel vehicles, with emission factors being three
399 orders of magnitude higher than those from gasoline vehicles. In addition, emission
400 factors of HCN from gasoline vehicles are similar to those from diesel vehicles. These
401 results are consistent with the measurements using the I⁻ ToF-CIMS from the same

402 campaign, as shown in Li et al. (2021).

403 The scatterplot shown in Fig. 8 can also be expressed in terms of the determined
404 fuel-based emission factors between gasoline and diesel vehicles (Fig. S10a).
405 Generally, similar variability is obtained except the determined slope of the data points,
406 with higher slopes determined from the scatterplot based on fuel-based emission factor
407 (0.19 versus 0.15). The emission ratios to CO between gasoline and diesel vehicles
408 (Fig. S10b) show similar results. Furthermore, the difference between the slopes
409 reflects the different average mileage for the same weight of fuel between gasoline
410 ($9.7 \text{ km}\cdot\text{kg}_{\text{fuel}}^{-1}$) and diesel vehicles ($7.1 \text{ km}\cdot\text{kg}_{\text{fuel}}^{-1}$), as demonstrated for emission
411 factors of CO₂ in Table S6.

412 Comparing gasoline and diesel vehicles, we can also observe profound
413 differences in relative changes of emission factors for analogous compounds series. The
414 emission factors of C₆-C₁₀ aromatics are apparently higher for gasoline vehicles than
415 diesel vehicles, whereas emission factors for larger aromatics ($n_c > 11$) from diesel
416 vehicles start to exceed gasoline vehicles. This interesting behavior is the result of
417 different variations of emission factors for gasoline and diesel vehicles as carbon
418 number increases. This may be attributed to the differences of chemical compositions
419 of gasoline and diesel fuel, such as higher fractions of polycyclic aromatic
420 hydrocarbons (PAHs) in the diesel fuel (Yue et al., 2015; Gentner et al., 2017). As shown
421 in Fig. 9, emission factors of aromatics from gasoline vehicles start to rapidly decrease
422 at $n_c = 10$ (a factor of 5 for each additional carbon for C₁₀-C₁₅), while the emission
423 factors of aromatic for diesel vehicles demonstrate a relatively flat pattern between C₆
424 and C₁₅, only with significant decrease for $n_c > 15$. Based on Fig. 9, we determine that
425 emissions of aromatics with $n_c \geq 10$ in gasoline and diesel vehicles account for 14% and
426 63% of total aromatic emissions, respectively, again suggesting the importance of
427 heavier aromatics in emissions from diesel vehicles. It also highlights that
428 quantification of these heavier species by PTR-ToF-MS may be important in
429 characterization of vehicular exhausts, especially diesel vehicles.

430 In addition to aromatics, the relative changes of emission factors for carbonyls
431 with carbon number are apparently different between gasoline and diesel vehicles (Fig.

432 8 and Fig. 9b). Emission factors of carbonyls tend to decrease as carbon number
433 increases for both gasoline and diesel vehicles. The extent of this decrease is observed
434 to be comparable for C₁-C₆ carbonyls in gasoline (97.6%) and diesel vehicles (97.4%).
435 However, as $n_c > 6$, the decrease in carbonyl emission factors for diesel vehicles
436 become smaller, resulting in larger emissions factors than gasoline vehicles for this
437 range of carbon number.

438 The above discussions demonstrate that emission characteristics of aromatics and
439 OVOCs are significantly different between gasoline and diesel vehicles. As the result,
440 the ratios of VOC pairs can be used to distinguish emissions of gasoline and diesel
441 vehicles. Fig. 10 shows the scatterplots of four representative VOCs (benzene, C₁₄
442 aromatics, formaldehyde, and acetaldehyde) versus toluene based on the determined
443 emission factors. The data points for each VOCs pair clearly show distinct separation
444 between gasoline vehicles and diesel vehicles, with apparently higher slopes for diesel
445 vehicles than gasoline vehicles, as the result of much larger emission factors of toluene
446 from gasoline vehicles and lower emission factors of the four representative VOCs
447 from diesel vehicles. The benzene/toluene ratio in gasoline and diesel vehicle are
448 determined as 0.48 and 1.24 mg·mg⁻¹ (corresponding to 0.57 and 1.46 ppb·ppb⁻¹ that
449 are more widely used in ambient studies). The difference of benzene/toluene ratio
450 between gasoline and diesel vehicles has been reported in previous studies, and our
451 results are generally consistent with these previous results (Chan et al., 2002; Barletta
452 et al., 2005; Qiao et al., 2012; Kumar et al., 2020). Compared to benzene/toluene ratio,
453 the difference of C₁₄ aromatics/toluene ratio between gasoline and diesel vehicles are
454 more substantial (a factor of 3800). The significantly higher emission factors of C₁₄
455 aromatics from diesel vehicles suggest that diesel vehicles can be a significant or even
456 dominant source of higher molecular-weight aromatics. The enormous difference of
457 C₁₄ aromatics/toluene ratio (and also other higher aromatics/toluene) between gasoline
458 and diesel vehicles indicate these ratios could potentially provide good indicators for
459 separation of gasoline and diesel vehicles in ambient or tunnel studies (see discussion
460 in Sect. 5 in the Supplement for details about the feasibility of the ratio using in
461 ambient air). Similar discrepancies are observed for formaldehyde/toluene and

462 acetaldehyde/toluene ratios between gasoline and diesel vehicles. These ratios may
463 not be able to be used as indicators to distinguish gasoline and diesel vehicles in
464 ambient studies, since secondary sources may complicate the observed ratios in
465 ambient air. However, these results strongly suggest that diesel vehicles can be
466 important in emissions of these OVOC species, though the number of diesel vehicles
467 are smaller than gasoline vehicles in many countries, e.g. China and U.S (Wallington
468 et al., 2013; Yao et al., 2015; Huang et al., 2021).

469 **3.4 OVOC fractions in VOC emissions**

470 Emission factors of various VOC species measured by PTR-ToF-MS from
471 different vehicles are summarized in Fig. 11. As shown in Fig. 11a, the determined
472 average mileage-based emission factors of total VOC ions from diesel vehicles were
473 much higher than gasoline and LPG vehicles. Fig. 11b-d quantified the proportions of
474 different categories of ions measured by PTR-ToF-MS. The determined average
475 mileage-based emission factors of C_xH_y accounted for the largest fraction in gasoline
476 vehicles ($84\% \pm 5.9\%$), and lower fractions in diesel ($47\% \pm 16\%$) and LPG vehicles
477 ($32\% \pm 0.7\%$). OVOCs account for larger fractions in diesel ($49\% \pm 16\%$) and LPG
478 vehicles ($58\% \pm 3.7\%$), while they only account for $13\% \pm 6.1\%$ of emissions from
479 gasoline vehicles. The fractions of different OVOC groups generally demonstrate a
480 downward trend from $C_xH_yO_1$ to $C_xH_yO_{\geq 3}$, and OVOCs with more than two oxygen
481 atoms only occupy small percentages (0-7%) in vehicle exhausts, indicating low
482 emissions of these species.

483 Combined with measurements of other VOCs from canisters measured by GC-
484 MS/FID, the fractions of OVOCs in total VOC emissions can be determined for
485 different vehicles (details in Sect. 6 in the Supplement) (Fig. 12). OVOCs account for
486 $9.4\% \pm 5.6\%$ of total VOC emissions for gasoline vehicles. The OVOC fractions for
487 gasoline vehicles are generally comparable for different emission standards and
488 cold/hot start, except somewhat higher fractions for China VI from hot start (Fig. S11).
489 The OVOC fractions obtained in this study for gasoline vehicles are generally
490 consistent with previous results (Cao et al., 2016; Wang et al., 2020b) (Fig. 12). Among

491 these studies, the OVOC fractions determined for gasoline with 10% ethanol (E10)
492 (Roy et al., 2016) ($22\% \pm 11\%$) are apparently higher. The fractions of OVOCs in total
493 VOC emissions for diesel vehicles are $71\% \pm 20\%$, $65\% \pm 22\%$, $52\% \pm 18\%$, and 56%
494 $\pm 26\%$ for LDDT, MDDT, HDDT, and bus, respectively. The variations of OVOC
495 fractions with emission standards are observed to be mixed among different types of
496 diesel vehicles (Fig. S11). The OVOC fractions from diesel vehicles are obviously
497 higher than those in gasoline vehicles, indicating the importance of OVOCs in VOC
498 emissions from diesel vehicles. Compared to previous studies (Tsai et al., 2012; Qiao et
499 al., 2012; Cao et al., 2016; Mo et al., 2016), determined OVOC fractions for diesel
500 vehicles in this study are higher. If only considering carbonyls among various types of
501 OVOCs measured by PTR-ToF-MS, the OVOC fractions determined in this study are
502 more comparable with previous studies (Fig. 12), since most previous studies only
503 detected carbonyls among various types of OVOCs. Finally, we determine that OVOCs
504 account for $41\% \pm 10\%$ of total VOC emissions for LPG vehicles, which is also higher
505 than a previous study (Wang et al., 2020b) where only carbonyls and a few
506 esters/alcohols were included. These results stress that the large number of OVOCs
507 measured by PTR-ToF-MS are important in characterization of VOC emissions from
508 vehicles. It should be noted that the OVOC fractions obtained here only reflect exhaust
509 emissions. Evaporative emissions may also be associated with different fractions of
510 various VOC groups, which may be more related to fuel compositions (Rubin et al.,
511 2006; Huang et al., 2021).

512 **4. Conclusions**

513 In this work, we conducted a chassis dynamometer study to measure VOC
514 emissions from gasoline, diesel, and LPG vehicles using PTR-ToF-MS along with other
515 offline and online measurement techniques. Using this dataset, we provide emission
516 factors of many VOCs from these three different types of vehicles associated with
517 various emission standards in China. Our results show that emission factors of VOCs
518 generally decrease with the increased stringency of emission standards for gasoline
519 vehicles, whereas variations of emission factors for diesel vehicles with emission

520 standards are more diverse. Mass spectra analysis of PTR-ToF-MS suggest that cold
521 start significantly influence VOCs emission of gasoline vehicles, while the influences
522 are smaller for diesel vehicles.

523 We observe large differences of VOC emissions between gasoline and diesel
524 vehicles based on PTR-ToF-MS measurements. Emission factors of most VOC species
525 from diesel vehicles were higher than gasoline vehicles, especially for most OVOCs
526 and heavier aromatics. The substantially larger emission factors of some OVOCs
527 emission factors for diesel vehicles indicate potentially dominant emissions of these
528 species from diesel vehicles among vehicular emissions. Our results suggest that VOC
529 pairs (e.g. C₁₄ aromatics/toluene ratio) could potentially provide good indicators for
530 distinguishing emissions between gasoline and diesel vehicles.

531 Based on measurements of PTR-ToF-MS, C_xH_y ions account for the largest
532 fraction in gasoline vehicles (84% ± 5.9%), whereas OVOC ions are the largest
533 contributor in the mass spectra of emissions from diesel (49% ± 16%) and LPG vehicles
534 (58% ± 3.7%). In the end, the fractions of OVOCs in total VOC emissions are
535 determined by combining hydrocarbons measurements from canister results and online
536 measurements of PTR-ToF-MS. We show that OVOCs contribute 9.4% ± 5.6% of the
537 total VOC emissions from gasoline vehicles, while the fractions are significantly higher
538 for diesel vehicles (52-71%), highlighting the importance to measure these OVOC
539 species in diesel emissions.

540 This study shows significant contributions of OVOCs in VOC emissions from
541 various vehicles, especially diesel vehicles. As a consequence, vehicular emissions may
542 account for considerable proportions for primary emissions of these OVOCs in urban
543 regions. Emissions of many OVOC species are currently not fully represented in
544 emission inventories of VOCs, which may in turn affect the prediction ability of air
545 quality models in urban regions. In this study, OVOC species are mainly quantified
546 from PTR-ToF-MS measurements by taking into account all signals in the mass spectra,
547 which stress that the large number of OVOC species measured by PTR-ToF-MS are
548 important in characterization of VOC emissions from vehicles.

549 **Data availability**

550 Data are available from the authors upon request.

551 **Author contribution**

552 BY designed the research. ZBY, BY, QES organized vehicle test measurements.
553 SHW, CHW, CMW, TGL, JPQ, QES, and MMZ contributed to data collection. SHW
554 performed the data analysis, with contributions from TGL, XJH, YBH, XBL, and QES.
555 SHW and BY prepared the manuscript with contributions from other authors. All the
556 authors reviewed the manuscript.

557 **Competing interests**

558 The authors declare that they have no known competing financial interests or
559 personal relationships that could have appeared to influence the work reported in this
560 paper.

561 **Acknowledgement**

562 This work was supported by the National Key R&D Plan of China (grant No.
563 2019YFE0106300, 2018YFC0213904), the National Natural Science Foundation of
564 China (grant No. 41877302, 42121004), Guangdong Natural Science Funds for
565 Distinguished Young Scholar (grant No. 2018B030306037), Guangdong Basic and
566 Applied Basic Research Fund Project (grant No. 2020A1515110085), and Guangdong
567 Innovative and Entrepreneurial Research Team Program (grant No. 2016ZT06N263).
568 This work was also supported by Special Fund Project for Science and Technology
569 Innovation Strategy of Guangdong Province (Grant No.2019B121205004). TK and
570 MG were supported by OEAD grant CN 05/2020. The authors would like to thank Prof.
571 Junyu Zheng for providing many resources during vehicle measurements and allowing
572 to use PEMS and formaldehyde data in this study.

573

574 **References**

- 575 Permissible Exposure Levels for Selected Military Fuel Vapors, The National
576 Academies Press, Washington, DC, 1996.
- 577 Barletta, B., Meinardi, S., Sherwood Rowland, F., Chan, C.-Y., Wang, X., Zou, S., Yin
578 Chan, L., and Blake, D. R.: Volatile organic compounds in 43 Chinese cities,
579 Atmospheric Environment, 39, 5979-5990, 10.1016/j.atmosenv.2005.06.029, 2005.
- 580 Cao, X., Yao, Z., Shen, X., Ye, Y., and Jiang, X.: On-road emission characteristics of
581 VOCs from light-duty gasoline vehicles in Beijing, China, Atmospheric Environment,
582 124, 146-155, 10.1016/j.atmosenv.2015.06.019, 2016.
- 583 Cappellin, L., Karl, T., Probst, M., Ismailova, O., Winkler, P. M., Soukoulis, C., Aprea,
584 E., Mark, T. D., Gasperi, F., and Biasioli, F.: On quantitative determination of volatile
585 organic compound concentrations using proton transfer reaction time-of-flight mass
586 spectrometry, Environmental Science & Technology, 46, 2283-2290,
587 10.1021/es203985t, 2012.
- 588 Chan, C. Y., Chan, L. Y., Wang, X. M., Liu, Y. M., Lee, S. C., Zou, S. C., Sheng, G. Y.,
589 and Fu, J. M.: Volatile organic compounds in roadside microenvironments of
590 metropolitan Hong Kong, Atmospheric Environment, 36, 2039-2047,
591 [https://doi.org/10.1016/S1352-2310\(02\)00097-3](https://doi.org/10.1016/S1352-2310(02)00097-3), 2002.
- 592 Cui, L., Wang, X. L., Ho, K. F., Gao, Y., Liu, C., Hang Ho, S. S., Li, H. W., Lee, S. C.,
593 Wang, X. M., Jiang, B. Q., Huang, Y., Chow, J. C., Watson, J. G., and Chen, L.-W.:
594 Decrease of VOC emissions from vehicular emissions in Hong Kong from 2003 to 2015:
595 Results from a tunnel study, Atmospheric Environment, 177, 64-74,
596 10.1016/j.atmosenv.2018.01.020, 2018.
- 597 Drozd, G. T., Zhao, Y., Saliba, G., Frodin, B., Maddox, C., Weber, R. J., Chang, M. O.,
598 Maldonado, H., Sardar, S., Robinson, A. L., and Goldstein, A. H.: Time Resolved
599 Measurements of Speciated Tailpipe Emissions from Motor Vehicles: Trends with
600 Emission Control Technology, Cold Start Effects, and Speciation, Environmental
601 Science & Technology, 50, 13592-13599, 10.1021/acs.est.6b04513, 2016.
- 602 Drozd, G. T., Zhao, Y., Saliba, G., Frodin, B., Maddox, C., Oliver Chang, M. C.,
603 Maldonado, H., Sardar, S., Weber, R. J., Robinson, A. L., and Goldstein, A. H.: Detailed
604 Speciation of Intermediate Volatility and Semivolatile Organic Compound Emissions
605 from Gasoline Vehicles: Effects of Cold-Starts and Implications for Secondary Organic
606 Aerosol Formation, Environ Sci Technol, 53, 1706-1714, 10.1021/acs.est.8b05600,
607 2019.
- 608 Erickson, M. H., Gueneron, M., and Jobson, B. T.: Measuring long chain alkanes in
609 diesel engine exhaust by thermal desorption PTR-MS, Atmospheric Measurement
610 Techniques, 7, 225-239, 10.5194/amt-7-225-2014, 2014.
- 611 Gentner, D. R., Isaacman, G., Worton, D. R., Chan, A. W., Dallmann, T. R., Davis, L.,
612 Liu, S., Day, D. A., Russell, L. M., Wilson, K. R., Weber, R., Guha, A., Harley, R. A.,
613 and Goldstein, A. H.: Elucidating secondary organic aerosol from diesel and gasoline
614 vehicles through detailed characterization of organic carbon emissions, Proc Natl Acad
615 Sci U S A, 109, 18318-18323, 10.1073/pnas.1212272109, 2012.

616 Gentner, D. R., Worton, D. R., Isaacman, G., Davis, L. C., Dallmann, T. R., Wood, E.
617 C., Herndon, S. C., Goldstein, A. H., and Harley, R. A.: Chemical Composition of Gas-
618 Phase Organic Carbon Emissions from Motor Vehicles and Implications for Ozone
619 Production, *Environmental Science & Technology*, 47, 11837-11848,
620 10.1021/es401470e, 2013.

621 Gentner, D. R., Jathar, S. H., Gordon, T. D., Bahreini, R., Day, D. A., El Haddad, I.,
622 Hayes, P. L., Pieber, S. M., Platt, S. M., de Gouw, J., Goldstein, A. H., Harley, R. A.,
623 Jimenez, J. L., Prevot, A. S., and Robinson, A. L.: Review of Urban Secondary Organic
624 Aerosol Formation from Gasoline and Diesel Motor Vehicle Emissions, *Environ Sci*
625 *Technol*, 51, 1074-1093, 10.1021/acs.est.6b04509, 2017.

626 George, I. J., Hays, M. D., Herrington, J. S., Preston, W., Snow, R., Faircloth, J., George,
627 B. J., Long, T., and Baldauf, R. W.: Effects of Cold Temperature and Ethanol Content
628 on VOC Emissions from Light-Duty Gasoline Vehicles, *Environ Sci Technol*, 49,
629 13067-13074, 10.1021/acs.est.5b04102, 2015.

630 Guo, H., Zou, S. C., Tsai, W. Y., Chan, L. Y., and Blake, D. R.: Emission characteristics
631 of nonmethane hydrocarbons from private cars and taxis at different driving speeds in
632 Hong Kong, *Atmospheric Environment*, 45, 2711-2721,
633 10.1016/j.atmosenv.2011.02.053, 2011.

634 Han, C., Liu, R., Luo, H., Li, G., Ma, S., Chen, J., and An, T.: Pollution profiles of
635 volatile organic compounds from different urban functional areas in Guangzhou China
636 based on GC/MS and PTR-TOF-MS: Atmospheric environmental implications,
637 *Atmospheric Environment*, 214, 10.1016/j.atmosenv.2019.116843, 2019.

638 He, X., Yuan, B., Wu, C., Wang, S., Wang, C., Huangfu, Y., Qi, J., Ma, N., Xu, W.,
639 Wang, M., Chen, W., Su, H., Cheng, Y., and Shao, M.: Volatile organic compounds in
640 wintertime North China Plain: Insights from measurements of proton transfer reaction
641 time-of-flight mass spectrometer (PTR-ToF-MS), *Journal of Environmental Sciences*,
642 10.1016/j.jes.2021.08.010, 2022.

643 Huang, J., Yuan, Z., Duan, Y., Liu, D., Fu, Q., Liang, G., Li, F., and Huang, X.:
644 Quantification of temperature dependence of vehicle evaporative volatile organic
645 compound emissions from different fuel types in China, *Sci Total Environ*, 813, 152661,
646 10.1016/j.scitotenv.2021.152661, 2021.

647 http://e.jmrb.com/m/2008/11/17/10/m_182226.shtml, Access on 2009-12-10, 2008.

648 Kansal, A.: Sources and reactivity of NMHCs and VOCs in the atmosphere: a review,
649 *J Hazard Mater*, 166, 17-26, 10.1016/j.jhazmat.2008.11.048, 2009.

650 Koss, A. R., Sekimoto, K., Gilman, J. B., Selimovic, V., Coggon, M. M., Zarzana, K.
651 J., Yuan, B., Lerner, B. M., Brown, S. S., Jimenez, J. L., Krechmer, J., Roberts, J. M.,
652 Warneke, C., Yokelson, R. J., and de Gouw, J.: Non-methane organic gas emissions
653 from biomass burning: identification, quantification, and emission factors from PTR-
654 ToF during the FIREX 2016 laboratory experiment, *Atmospheric Chemistry and*
655 *Physics*, 18, 3299-3319, 10.5194/acp-18-3299-2018, 2018.

656 Kroll, J. H., Donahue, N. M., Jimenez, J. L., Kessler, S. H., Canagaratna, M. R., Wilson,
657 K. R., Altieri, K. E., Mazzoleni, L. R., Wozniak, A. S., Bluhm, H., Mysak, E. R., Smith,
658 J. D., Kolb, C. E., and Worsnop, D. R.: Carbon oxidation state as a metric for describing

659 the chemistry of atmospheric organic aerosol, *Nat Chem*, 3, 133-139,
660 10.1038/nchem.948, 2011.

661 Kumar, A., Sinha, V., Shabin, M., Hakkim, H., Bonsang, B., and Gros, V.: Non-methane
662 hydrocarbon (NMHC) fingerprints of major urban and agricultural emission sources for
663 use in source apportionment studies, *Atmospheric Chemistry and Physics*, 20, 12133-
664 12152, 10.5194/acp-20-12133-2020, 2020.

665 Laurikko, J.: Ambient temperature effect on automotive exhaust emissions: FTP and
666 ECE test cycle responses, *The Science of Environment*, 169, 195-204, 1995.

667 Li, B., Ho, S. S. H., Xue, Y., Huang, Y., Wang, L., Cheng, Y., Dai, W., Zhong, H., Cao,
668 J., and Lee, S.: Characterizations of volatile organic compounds (VOCs) from vehicular
669 emissions at roadside environment: The first comprehensive study in Northwestern
670 China, *Atmospheric Environment*, 161, 1-12, 10.1016/j.atmosenv.2017.04.029, 2017.

671 Li, T., Wang, Z., Yuan, B., Ye, C., Lin, Y., Wang, S., Sha, Q. e., Yuan, Z., Zheng, J., and
672 Shao, M.: Emissions of carboxylic acids, hydrogen cyanide (HCN) and isocyanic acid
673 (HNCO) from vehicle exhaust, *Atmospheric Environment*,
674 10.1016/j.atmosenv.2021.118218, 2021.

675 Li, X., Wu, Y., Yao, X., Zhang, S., Zhou, Y., and Fu, L.: Evaluation of the environmental
676 benefits of the enhanced vehicle inspection /maintenance program based on the short
677 transient loaded mode in Guangzhou (in Chinese), *Acta Scientiae Circumstantiae*, 32(1),
678 101-108, 10.13671/j.hjkxxb.2012.01.009, 2012.

679 Liao, S., Zhang, J., Yu, F., Zhu, M., Liu, J., Ou, J., Dong, H., Sha, Q., Zhong, Z., Xie,
680 Y., Luo, H., Zhang, L., and Zheng, J.: High Gaseous Nitrous Acid (HONO) Emissions
681 from Light-Duty Diesel Vehicles, *Environ Sci Technol*, 55, 200-208,
682 10.1021/acs.est.0c05599, 2021.

683 Liu, H., Man, H., Cui, H., Wang, Y., Deng, F., Wang, Y., Yang, X., Xiao, Q., Zhang, Q.,
684 Ding, Y., and He, K.: An updated emission inventory of vehicular VOCs and IVOCs in
685 China, *Atmospheric Chemistry and Physics*, 17, 12709-12724, 10.5194/acp-17-12709-
686 2017, 2017.

687 Liu, Y., Shao, M., Fu, L., Lu, S., Zeng, L., and Tang, D.: Source profiles of volatile
688 organic compounds (VOCs) measured in China: Part I, *Atmospheric Environment*, 42,
689 6247-6260, 10.1016/j.atmosenv.2008.01.070, 2008.

690 Liu, Y., Li, Y., Yuan, Z., Wang, H., Sha, Q., Lou, S., Liu, Y., Hao, Y., Duan, L., Ye, P.,
691 Zheng, J., Yuan, B., and Shao, M.: Identification of two main origins of intermediate-
692 volatility organic compound emissions from vehicles in China through two-phase
693 simultaneous characterization, *Environ Pollut*, 281, 117020,
694 10.1016/j.envpol.2021.117020, 2021.

695 Lu, Q., Zhao, Y., and Robinson, A. L.: Comprehensive organic emission profiles for
696 gasoline, diesel, and gas-turbine engines including intermediate and semi-volatile
697 organic compound emissions, *Atmospheric Chemistry and Physics*, 18, 17637-17654,
698 10.5194/acp-18-17637-2018, 2018.

699 Ly, B. T., Kajii, Y., Nguyen, T. Y., Shoji, K., Van, D. A., Do, T. N., Nghiem, T. D., and
700 Sakamoto, Y.: Characteristics of roadside volatile organic compounds in an urban area
701 dominated by gasoline vehicles, a case study in Hanoi, *Chemosphere*, 254, 126749,
702 10.1016/j.chemosphere.2020.126749, 2020.

703 Lyu, M., Bao, X., Zhu, R., and Matthews, R.: State-of-the-art outlook for light-duty
704 vehicle emission control standards and technologies in China, *Clean Technologies and*
705 *Environmental Policy*, 22, 757-771, 10.1007/s10098-020-01834-x, 2020.

706 May, A. A., Nguyen, N. T., Presto, A. A., Gordon, T. D., Lipsky, E. M., Karve, M.,
707 Gutierrez, A., Robertson, W. H., Zhang, M., Brandow, C., Chang, O., Chen, S., Cicero-
708 Fernandez, P., Dinkins, L., Fuentes, M., Huang, S.-M., Ling, R., Long, J., Maddox, C.,
709 Masetti, J., McCauley, E., Miguel, A., Na, K., Ong, R., Pang, Y., Rieger, P., Sax, T.,
710 Truong, T., Vo, T., Chattopadhyay, S., Maldonado, H., Maricq, M. M., and Robinson,
711 A. L.: Gas- and particle-phase primary emissions from in-use, on-road gasoline and
712 diesel vehicles, *Atmospheric Environment*, 88, 247-260,
713 10.1016/j.atmosenv.2014.01.046, 2014.

714 China Mobile Source Environmental Management Annual Report:
715 <http://www.mee.gov.cn/hjzl/sthjzk/ydyhjgl/201909/P020190905586230826402.pdf>,
716 2019.

717 Mo, Z., Shao, M., and Lu, S.: Compilation of a source profile database for hydrocarbon
718 and OVOC emissions in China, *Atmospheric Environment*, 143, 209-217,
719 10.1016/j.atmosenv.2016.08.025, 2016.

720 Ou, J., Zheng, J., Li, R., Huang, X., Zhong, Z., Zhong, L., and Lin, H.: Speciated OVOC
721 and VOC emission inventories and their implications for reactivity-based ozone control
722 strategy in the Pearl River Delta region, China, *Sci Total Environ*, 530-531, 393-402,
723 10.1016/j.scitotenv.2015.05.062, 2015.

724 Pang, X., Mu, Y., Yuan, J., and He, H.: Carbonyls emission from ethanol-blended
725 gasoline and biodiesel-ethanol-diesel used in engines, *Atmospheric Environment*, 42,
726 1349-1358, 10.1016/j.atmosenv.2007.10.075, 2008.

727 Parrish, D. D., Kuster, W. C., Shao, M., Yokouchi, Y., Kondo, Y., Goldan, P. D., de
728 Gouw, J. A., Koike, M., and Shirai, T.: Comparison of air pollutant emissions among
729 mega-cities, *Atmospheric Environment*, 43, 6435-6441,
730 10.1016/j.atmosenv.2009.06.024, 2009.

731 Qi, L., Liu, H., Shen, X., Fu, M., Huang, F., Man, H., Deng, F., Shaikh, A. A., Wang,
732 X., Dong, R., Song, C., and He, K.: Intermediate-Volatility Organic Compound
733 Emissions from Nonroad Construction Machinery under Different Operation Modes,
734 *Environ Sci Technol*, 53, 13832-13840, 10.1021/acs.est.9b01316, 2019.

735 Qiao, Y. Z., Wang, H. L., Huang, C., Chen, C. H., and Huang, H. Y.: Source profile and
736 chemical reactivity of volatile organic compounds from vehicle exhaust(in chinese),
737 *Environmental Science*, 33, 1071-1079, 2012.

738 Roy, A., Sonntag, D., Cook, R., Yanca, C., Schenk, C., and Choi, Y.: Effect of Ambient
739 Temperature on Total Organic Gas Speciation Profiles from Light-Duty Gasoline
740 Vehicle Exhaust, *Environmental Science & Technology*, 50, 6565-6573,
741 10.1021/acs.est.6b01081, 2016.

742 Rubin, J. I., Kean, A. J., Harley, R. A., Millet, D. B., and Goldstein, A. H.: Temperature
743 dependence of volatile organic compound evaporative emissions from motor vehicles,
744 *Journal of Geophysical Research: Atmospheres*, 111,
745 <https://doi.org/10.1029/2005JD006458>, 2006.

746 Schauer, J. J., Kleeman, M. J., Cass, G. R., and Simoneit, B. R., T.: Measurement of
747 Emissions from Air Pollution Sources. 2. C₁ through C₃₀ Organic Compounds from
748 Medium Duty Diesel Trucks, *Environmental Science & Technology*, 33, 1578-1587,
749 1999.

750 Seinfeld, J. H., and Pandis, S. N.: *Atmospheric chemistry and physics: from air
751 pollution to climate change*, John Wiley & Sons, Inc., Hoboken, 2006.

752 Sekimoto, K., Li, S.-M., Yuan, B., Koss, A., Coggon, M., Warneke, C., and de Gouw,
753 J.: Calculation of the sensitivity of proton-transfer-reaction mass spectrometry (PTR-
754 MS) for organic trace gases using molecular properties, *International Journal of Mass
755 Spectrometry*, 421, 71-94, 10.1016/j.ijms.2017.04.006, 2017.

756 Sha, Q., Zhu, M., Huang, H., Wang, Y., Huang, Z., Zhang, X., Tang, M., Lu, M., Chen,
757 C., Shi, B., Chen, Z., Wu, L., Zhong, Z., Li, C., Xu, Y., Yu, F., Jia, G., Liao, S., Cui, X.,
758 Liu, J., and Zheng, J.: A newly integrated dataset of volatile organic compounds (VOCs)
759 source profiles and implications for the future development of VOCs profiles in China,
760 *Sci Total Environ*, 793, 148348, 10.1016/j.scitotenv.2021.148348, 2021.

761 Shao, M., Zhang, Y., Zeng, L., Tang, X., Zhang, J., Zhong, L., and Wang, B.: Ground-
762 level ozone in the Pearl River Delta and the roles of VOC and NO_x in its production,
763 *Journal of Environmental Management*, 90, 512-518, 10.1016/j.jenvman.2007.12.008,
764 2009.

765 Shen, X., Lv, T., Zhang, X., Cao, X., Li, X., Wu, B., Yao, X., Shi, Y., Zhou, Q., Chen,
766 X., and Yao, Z.: Real-world emission characteristics of black carbon emitted by on-road
767 China IV and China V diesel trucks, *Science of The Total Environment*, 799, 149435,
768 <https://doi.org/10.1016/j.scitotenv.2021.149435>, 2021.

769 Song, C., Liu, Y., Sun, L., Zhang, Q., and Mao, H.: Emissions of volatile organic
770 compounds (VOCs) from gasoline- and liquified natural gas (LNG)-fueled vehicles in
771 tunnel studies, *Atmospheric Environment*, 234, 10.1016/j.atmosenv.2020.117626, 2020.

772 Stark, H., Yatavelli, R. L. N., Thompson, S. L., Kimmel, J. R., Cubison, M. J., Chhabra,
773 P. S., Canagaratna, M. R., Jayne, J. T., Worsnop, D. R., and Jimenez, J. L.: Methods to
774 extract molecular and bulk chemical information from series of complex mass spectra
775 with limited mass resolution, *International Journal of Mass Spectrometry*, 389, 26-38,
776 10.1016/j.ijms.2015.08.011, 2015.

777 Sulzer, P., Hartungen, E., Hanel, G., Feil, S., Winkler, K., Mutschlechner, P., Haidacher,
778 S., Schottkowsky, R., Gunsch, D., Seehauser, H., Striednig, M., Jürschik, S., Breiev, K.,
779 Lanza, M., Herbig, J., Märk, L., Märk, T. D., and Jordan, A.: A Proton Transfer
780 Reaction-Quadrupole interface Time-Of-Flight Mass Spectrometer (PTR-QiTOF):
781 High speed due to extreme sensitivity, *International Journal of Mass Spectrometry*, 368,
782 1-5, 10.1016/j.ijms.2014.05.004, 2014.

783 Sun, W., Shao, M., Granier, C., Liu, Y., Ye, C. S., and Zheng, J. Y.: Long-Term Trends
784 of Anthropogenic SO₂, NO_x, CO, and NMVOCs Emissions in China, *Earth's Future*, 6,
785 1112-1133, 10.1029/2018ef000822, 2018.

786 Tsai, J.-H., Chang, S.-Y., and Chiang, H.-L.: Volatile organic compounds from the
787 exhaust of light-duty diesel vehicles, *Atmospheric Environment*, 61, 499-506,
788 10.1016/j.atmosenv.2012.07.078, 2012.

789 Wallington, T. J., Lambert, C. K., and Ruona, W. C.: Diesel vehicles and sustainable
790 mobility in the U.S, *Energy Policy*, 54, 47-53, 10.1016/j.enpol.2011.11.068, 2013.

791 Wang, C., Yuan, B., Wu, C., Wang, S., Qi, J., Wang, B., Wang, Z., Hu, W., Chen, W.,
792 Ye, C., Wang, W., Sun, Y., Wang, C., Huang, S., Song, W., Wang, X., Yang, S., Zhang,
793 S., Xu, W., Ma, N., Zhang, Z., Jiang, B., Su, H., Cheng, Y., Wang, X., and Shao, M.:
794 Measurements of higher alkanes using NO⁺ chemical ionization in PTR-ToF-MS:
795 important contributions of higher alkanes to secondary organic aerosols in China,
796 *Atmospheric Chemistry and Physics*, 20, 14123-14138, 10.5194/acp-20-14123-2020,
797 2020a.

798 Wang, H., L. , Jing, S., A. , Lou, S., R. , Hu, Q., Y. , Li, L., Tao, S., K. , Huang, C., Qiao,
799 L., P. , and Chen, C., H.: Volatile organic compounds (VOCs) source profiles of on-
800 road vehicle emissions in China, *Sci Total Environ*, 607-608, 253-261,
801 10.1016/j.scitotenv.2017.07.001, 2017.

802 Wang, J., Jin, L., Gao, J., Shi, J., Zhao, Y., Liu, S., Jin, T., Bai, Z., and Wu, C. Y.:
803 Investigation of speciated VOC in gasoline vehicular exhaust under ECE and EUDC
804 test cycles, *Sci Total Environ*, 445-446, 110-116, 10.1016/j.scitotenv.2012.12.044, 2013.

805 Wang, M., Li, S., Zhu, R., Zhang, R., Zu, L., Wang, Y., and Bao, X.: On-road tailpipe
806 emission characteristics and ozone formation potentials of VOCs from gasoline, diesel
807 and liquefied petroleum gas fueled vehicles, *Atmospheric Environment*,
808 10.1016/j.atmosenv.2020.117294, 2020b.

809 Wang, Z., Yuan, B., Ye, C., Roberts, J., Wisthaler, A., Lin, Y., Li, T., Wu, C., Peng, Y.,
810 Wang, C., Wang, S., Yang, S., Wang, B., Qi, J., Wang, C., Song, W., Hu, W., Wang, X.,
811 Xu, W., Ma, N., Kuang, Y., Tao, J., Zhang, Z., Su, H., Cheng, Y., Wang, X., and Shao,
812 M.: High Concentrations of Atmospheric Isocyanic Acid (HNCO) Produced from
813 Secondary Sources in China, *Environmental Science & Technology*,
814 10.1021/acs.est.0c02843, 2020c.

815 Wu, C., Wang, C., Wang, S., Wang, W., Yuan, B., Qi, J., Wang, B., Wang, H., Wang, C.,
816 Song, W., Wang, X., Hu, W., Lou, S., Ye, C., Peng, Y., Wang, Z., Huangfu, Y., Xie, Y.,
817 Zhu, M., Zheng, J., Wang, X., Jiang, B., Zhang, Z., and Shao, M.: Measurement report:
818 Important contributions of oxygenated compounds to emissions and chemistry of
819 volatile organic compounds in urban air, *Atmospheric Chemistry and Physics*, 20,
820 14769-14785, 10.5194/acp-20-14769-2020, 2020.

821 Wu, R., Bo, Y., Li, J., Li, L., Li, Y., and Xie, S.: Method to establish the emission
822 inventory of anthropogenic volatile organic compounds in China and its application in
823 the period 2008–2012, *Atmospheric Environment*, 127, 244-254,
824 10.1016/j.atmosenv.2015.12.015, 2016.

825 Wu, Y., Zhang, S., Hao, J., Liu, H., Wu, X., Hu, J., Walsh, M. P., Wallington, T. J.,
826 Zhang, K. M., and Stevanovic, S.: On-road vehicle emissions and their control in China:
827 A review and outlook, *Sci Total Environ*, 574, 332-349,
828 10.1016/j.scitotenv.2016.09.040, 2017.

829 Yang, W., Zhang, Q., Wang, J., Zhou, C., Zhang, Y., and Pan, Z.: Emission
830 characteristics and ozone formation potentials of VOCs from gasoline passenger cars
831 at different driving modes, *Atmospheric Pollution Research*, 9, 804-813,
832 10.1016/j.apr.2018.01.002, 2018.

833 Yao, S., Liu, Z., and Qi, Z.: Test System for Exhaust Pollutants from Light-duty
834 Gasoline Vehicle under Short Transient Driving Cycle (in Chinese), Shanghai
835 Environmental Sciences, 10, 722-728, 2003.

836 Yao, Z., Shen, X., Ye, Y., Cao, X., Jiang, X., Zhang, Y., and He, K.: On-road emission
837 characteristics of VOCs from diesel trucks in Beijing, China, Atmospheric Environment,
838 103, 87-93, 10.1016/j.atmosenv.2014.12.028, 2015.

839 Ye, C., Yuan, B., Lin, Y., Wang, Z., Hu, W., Li, T., Chen, W., Wu, C., Wang, C., Huang,
840 S., Qi, J., Wang, B., Wang, C., Song, W., Wang, X., Zheng, E., Krechmer, J. E., Ye, P.,
841 Zhang, Z., Wang, X., Worsnop, D. R., and Shao, M.: Chemical characterization of
842 oxygenated organic compounds in the gas phase and particle phase using iodide CIMS
843 with FIGAERO in urban air, Atmospheric Chemistry and Physics, 21, 8455-8478,
844 10.5194/acp-21-8455-2021, 2021.

845 Yuan, B., Koss, A. R., Warneke, C., Coggon, M., Sekimoto, K., and de Gouw, J. A.:
846 Proton-Transfer-Reaction Mass Spectrometry: Applications in Atmospheric Sciences,
847 Chemical Reviews, 117, 13187-13229, 10.1021/acs.chemrev.7b00325, 2017.

848 Yue, X., Wu, Y., Hao, J., Pang, Y., Ma, Y., Li, Y., Li, B., and Bao, X.: Fuel quality
849 management versus vehicle emission control in China, status quo and future
850 perspectives, Energy Policy, 79, 87-98, <https://doi.org/10.1016/j.enpol.2015.01.009>,
851 2015.

852 Zavala, M., Herndon, S. C., Slott, R. S., Dunlea, E. J., Marr, L. C., Shorter, J. H.,
853 Zahniser, M., Knighton, W. B., Rogers, T. M., Kolb, C. E., Molina, L. T., and Molina,
854 M. J.: Characterization of on-road vehicle emissions in the Mexico City Metropolitan
855 Area using a mobile laboratory in chase and fleet average measurement modes during
856 the MCMA-2003 field campaign, Atmospheric Chemistry and Physics, 6, 5129-5142,
857 10.5194/acp-6-5129-2006, 2006.

858 Zavala, M., Herndon, S. C., Wood, E. C., Jayne, J. T., Nelson, D. D., Trimborn, A. M.,
859 Dunlea, E., Knighton, W. B., Mendoza, A., Allen, D. T., Kolb, C. E., Molina, M. J., and
860 Molina, L. T.: Comparison of emissions from on-road sources using a mobile laboratory
861 under various driving and operational sampling modes, Atmospheric Chemistry and
862 Physics, 9, 1-14, 10.5194/acp-9-1-2009, 2009.

863 Zhang, Q., Wu, L., Fang, X., Liu, M., Zhang, J., Shao, M., Lu, S., and Mao, H.:
864 Emission factors of volatile organic compounds (VOCs) based on the detailed vehicle
865 classification in a tunnel study, Sci Total Environ, 624, 878-886,
866 10.1016/j.scitotenv.2017.12.171, 2018.

867 Zhao, Y., Saleh, R., Saliba, G., Presto, A. A., Gordon, T. D., Drozd, G. T., Goldstein, A.
868 H., Donahue, N. M., and Robinson, A. L.: Reducing secondary organic aerosol
869 formation from gasoline vehicle exhaust, Proc Natl Acad Sci U S A, 114, 6984-6989,
870 10.1073/pnas.1620911114, 2017.

871 Zhou, H., Zhao, H., Hu, J., Li, M., Feng, Q., Qi, J., Shi, Z., Mao, H., and Jin, T.: Primary
872 particulate matter emissions and estimates of secondary organic aerosol formation
873 potential from the exhaust of a China V diesel engine, Atmospheric Environment, 218,
874 116987, <https://doi.org/10.1016/j.atmosenv.2019.116987>, 2019.

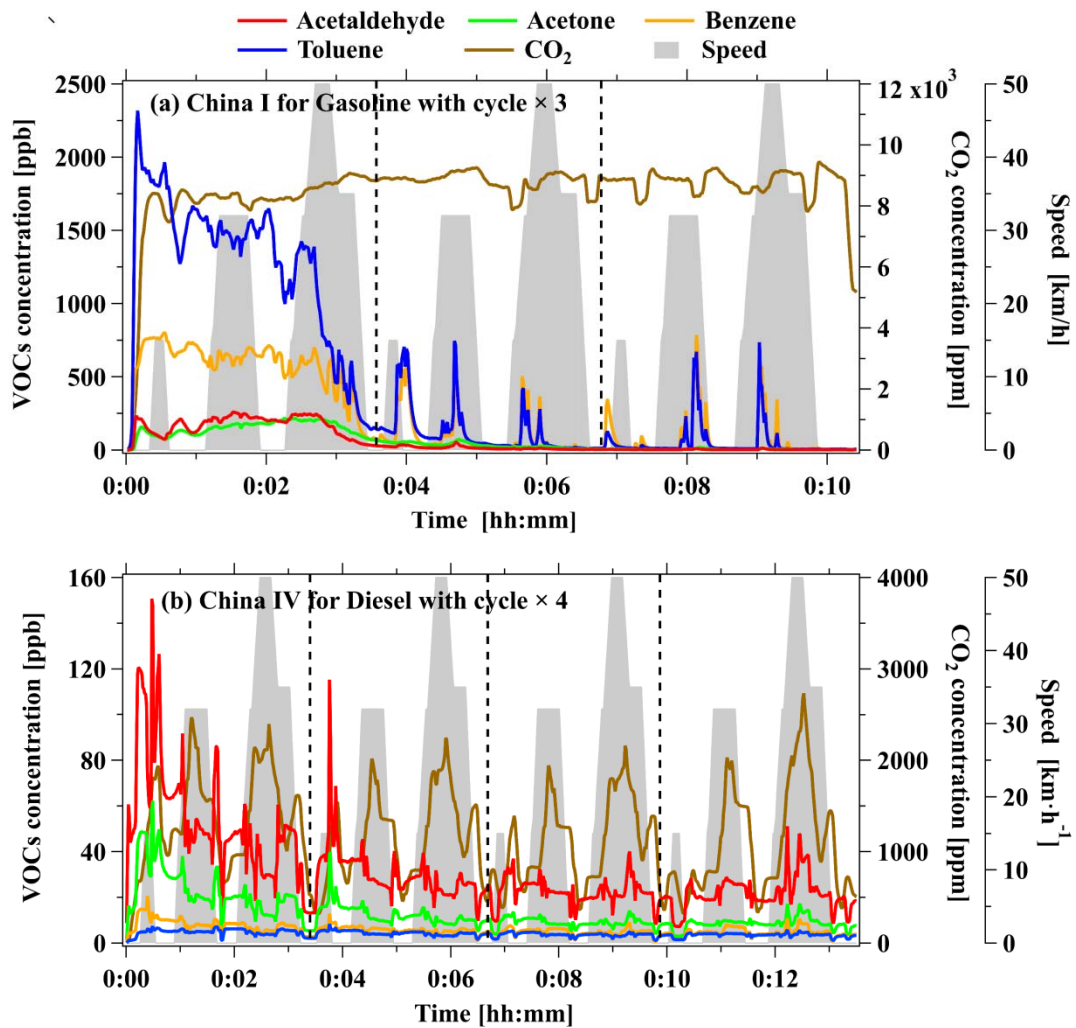
875 Zhu, M., Dong, H., Yu, F., Liao, S., Xie, Y., Liu, J., Sha, Q., Zhong, Z., Zeng, L., and
876 Zheng, J.: A New Portable Instrument for Online Measurements of Formaldehyde:

877 From Ambient to Mobile Emission Sources, *Environmental Science & Technology*
878 *Letters*, 7, 292-297, 10.1021/acs.estlett.0c00169, 2020.

879 Ziemann, P. J., and Atkinson, R.: Kinetics, products, and mechanisms of secondary
880 organic aerosol formation, *Chem Soc Rev*, 41, 6582-6605, 10.1039/c2cs35122f, 2012.

881

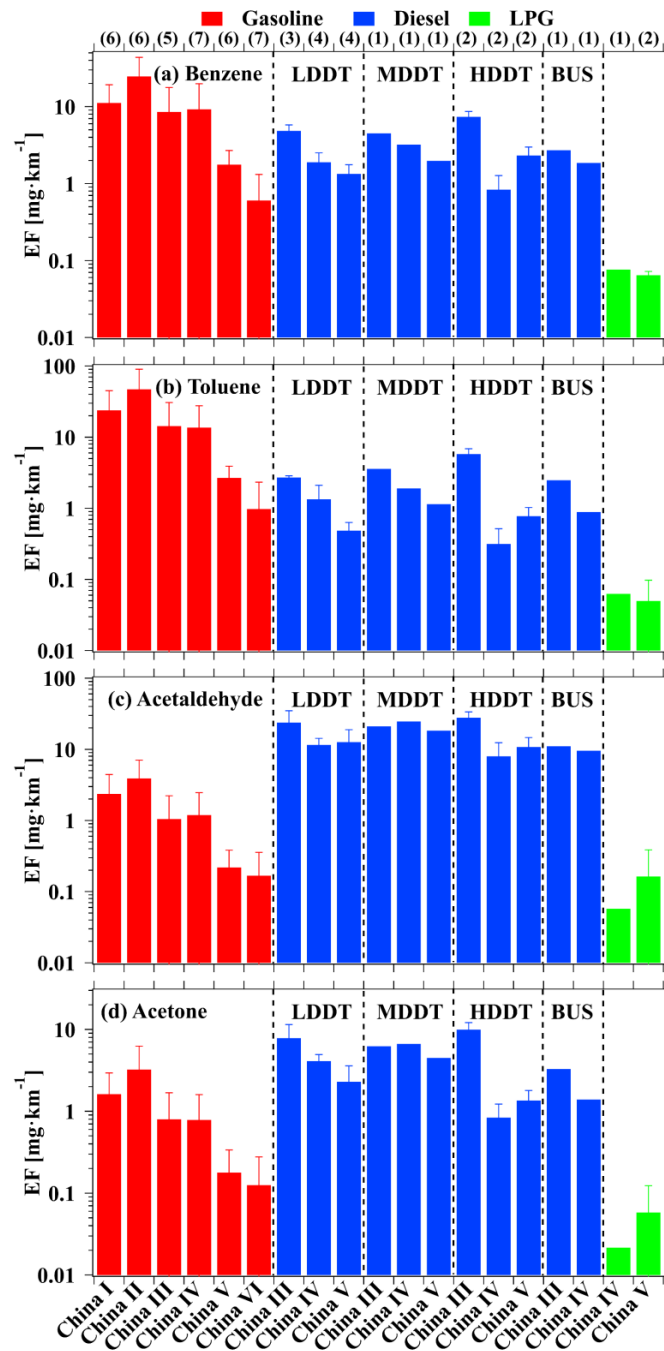
882



883

884 **Figure 1.** Real-time concentrations of acetaldehyde, acetone, benzene, toluene, and
 885 CO₂ for (a) a gasoline vehicle with emission standard of China I and (b) a light-duty
 886 diesel vehicle (LDDV) with emission standard of China IV. The two vehicles were both
 887 cold started. The gray shadows represent the speed of the vehicles on the chassis
 888 dynamometer.

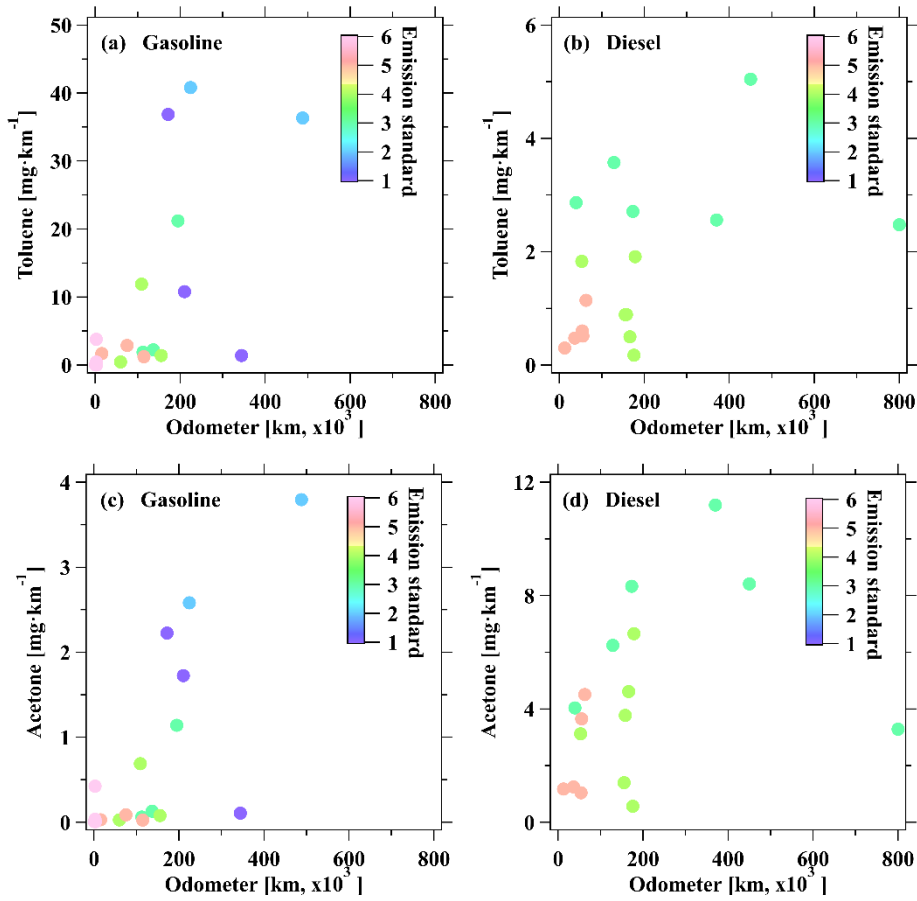
889



890

891 **Figure 2.** The determined average mileage-based emission factors ($\text{mg}\cdot\text{km}^{-1}$) for (a)
 892 benzene, (b) toluene, (c) acetaldehyde, and (d) acetone for vehicles with different
 893 emission standards. The numbers above the top axis represent the number of all
 894 experiments (including multiple measurements for individual test vehicle) for each
 895 emission standard. LDDT, MDDT, HDDT, and BUS represent light-duty-diesel-truck,
 896 middle-duty-diesel-truck, heavy-duty-diesel-truck, and bus, respectively. Error bars
 897 represent standard deviations of emission factors for the specific emission standard.

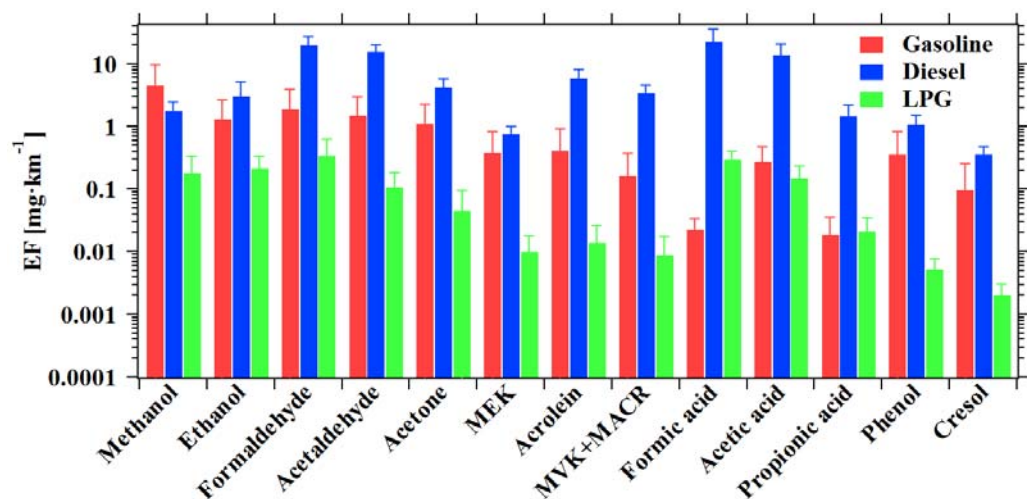
898



899

900 **Figure 3.** Scatterplot of the emission factor of toluene in (a) gasoline and (b) diesel
 901 vehicles, and acetone in (c) gasoline and (d) diesel vehicles during the hot start based
 902 on the odometer for each vehicle.

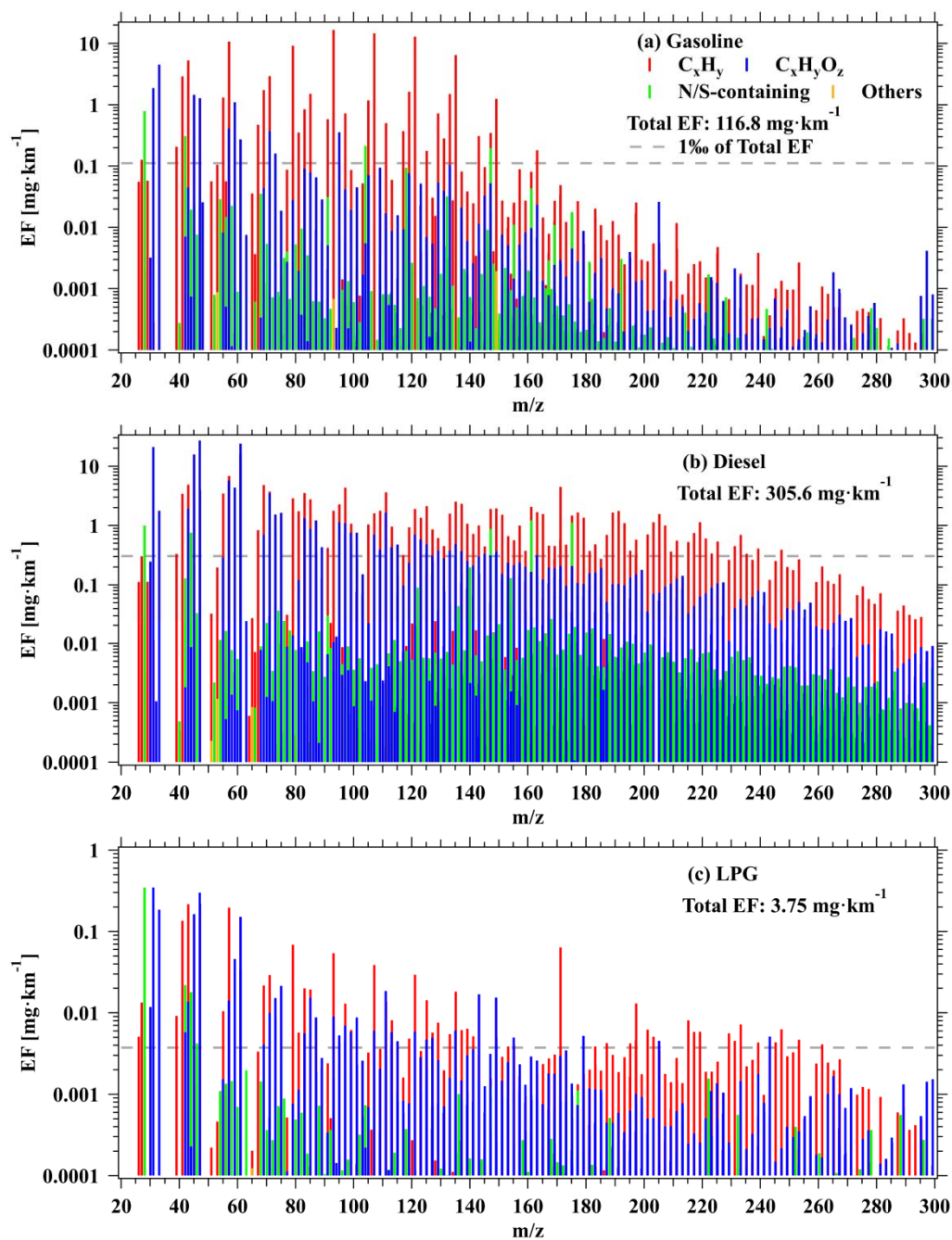
903



904

905 **Figure 4.** The determined emission factors of representative OVOC species from
 906 different types of vehicles. Error bars represent standard deviations of the emission
 907 factors for the VOCs.

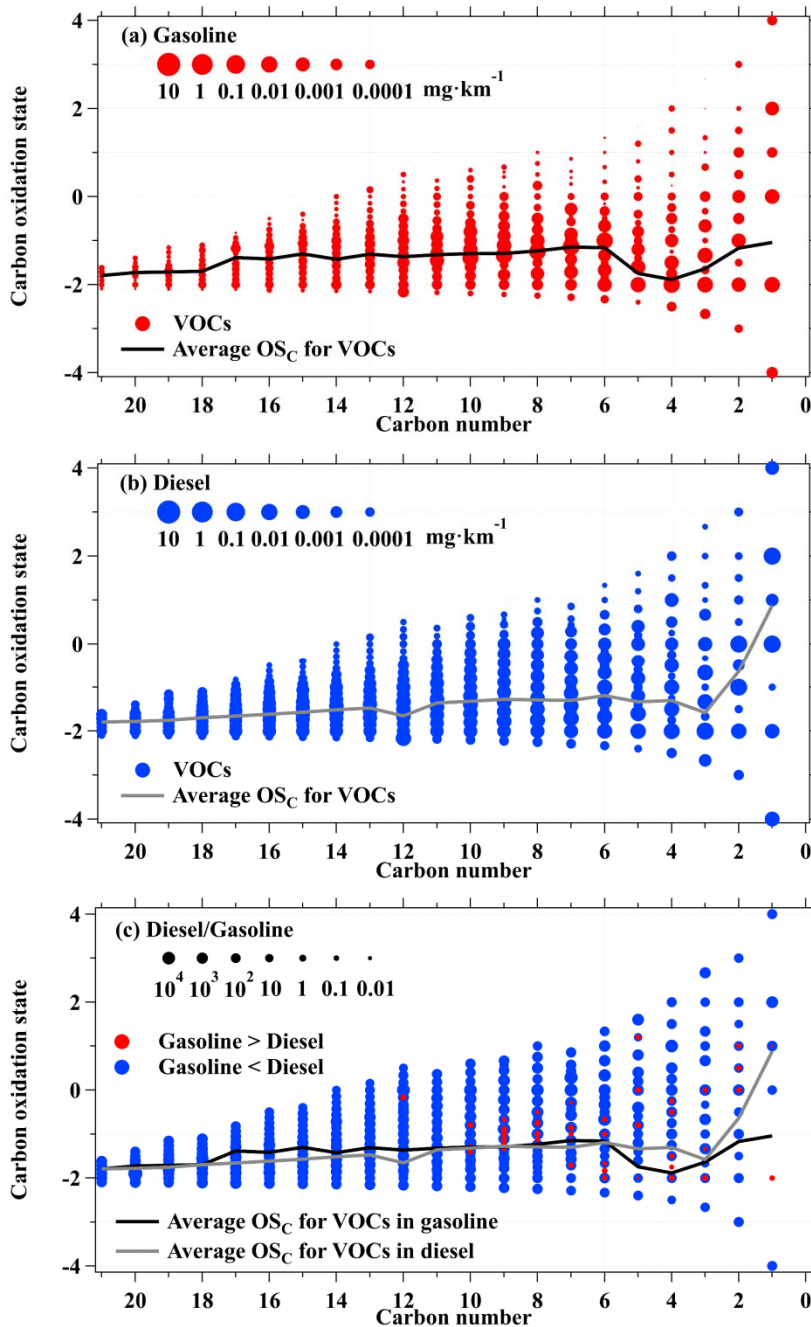
908



909

910 **Figure 5.** The determined average mileage-based emission factors of VOC species
 911 measured by PTR-ToF-MS from (a) gasoline, (b) diesel, and (c) LPG vehicles. The
 912 gray dashed lines represent 1% of total VOCs emission factors.

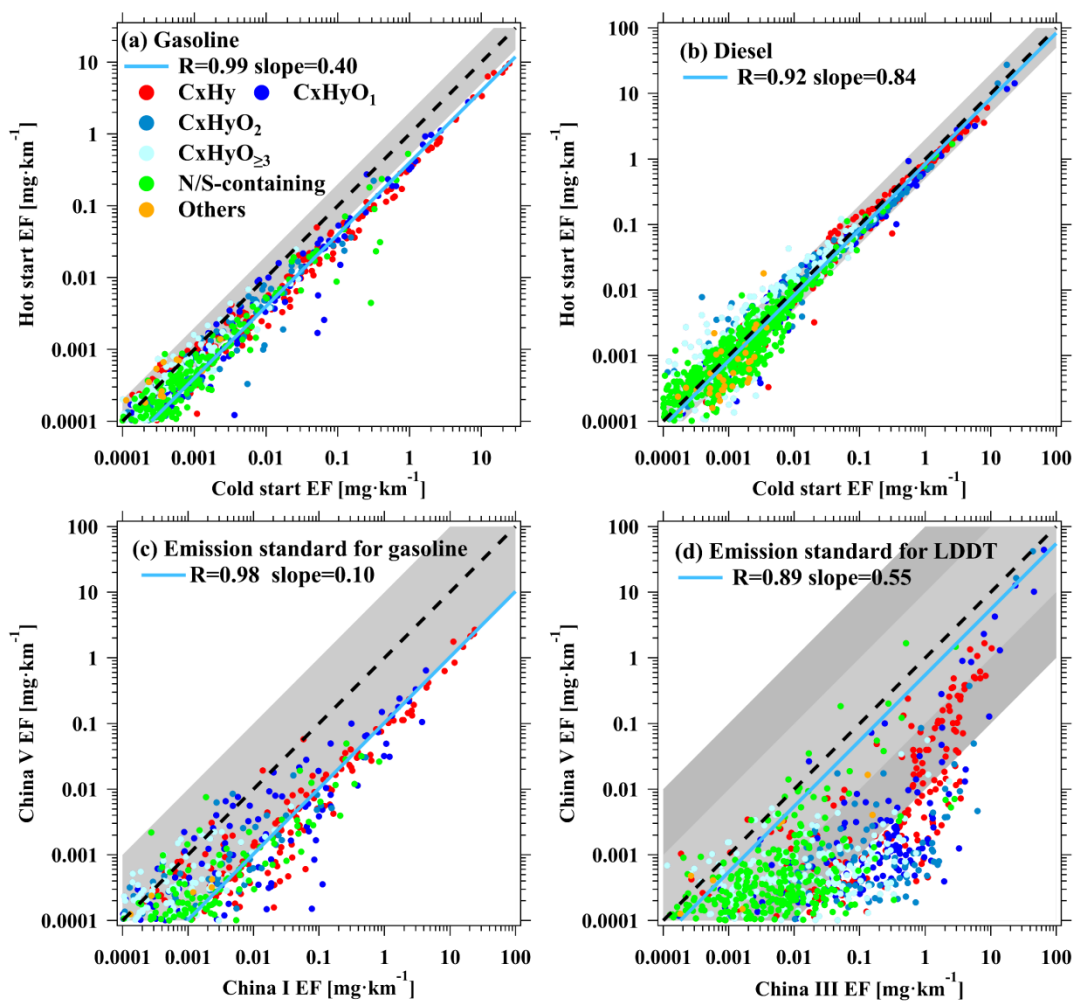
913



914

915 **Figure 6.** The two-dimensional space of $\overline{OS}_C - n_C$ with data points sized coded using
 916 emission factors of VOC species from (a) gasoline and (b) diesel vehicles, and (c) the
 917 ratio of emission factors of diesel vehicle relative to gasoline vehicle. The black and
 918 gray lines are the average \overline{OS}_C of each carbon number for VOC species in gasoline and
 919 diesel vehicles, respectively.

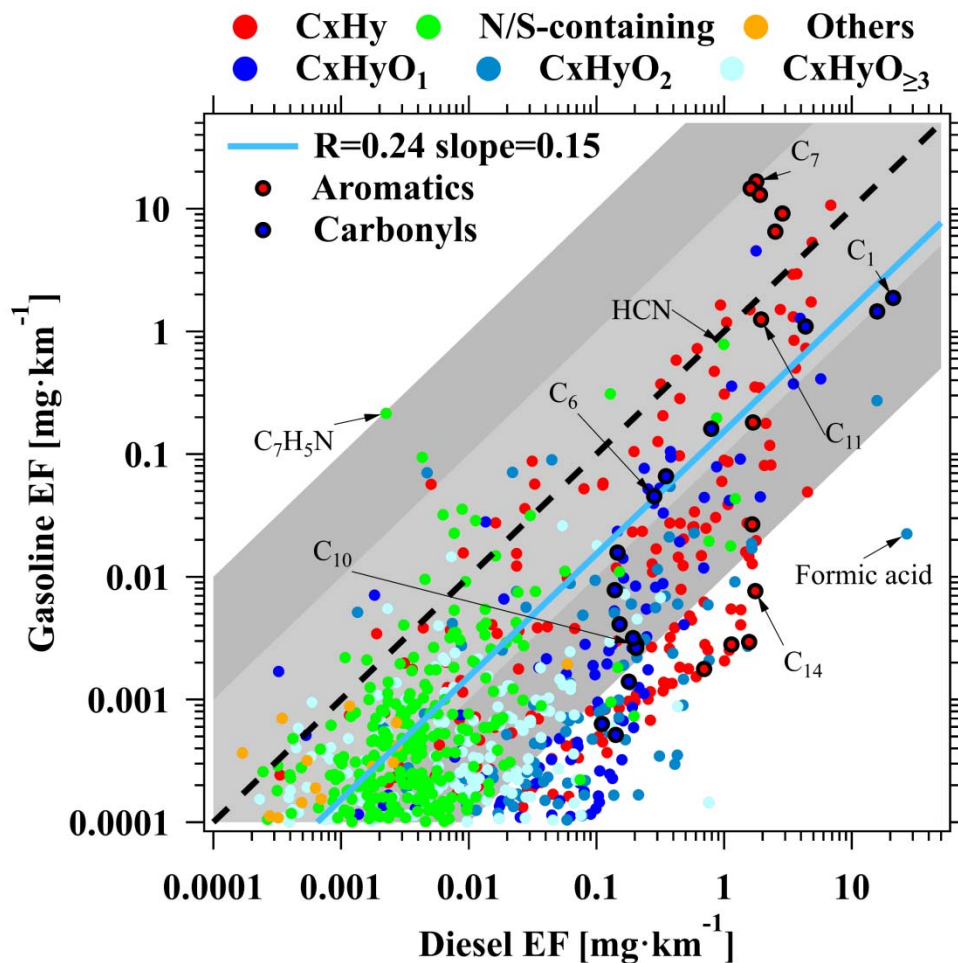
920



921

922 **Figure 7.** Scatterplots of VOCs emission factors between cold start and hot start for
 923 gasoline (a) and diesel vehicles (b). Scatterplots of VOCs emission factors between
 924 China I and China V emission standard for gasoline vehicles (c) and between China III
 925 and China V emission standard for diesel vehicles (d). Each data point indicates a VOC
 926 species measured by PTR-ToF-MS. The blue lines are the fitted results for all data
 927 points. The black dashed lines represent 1:1 ratio, and the shaded areas represent ratios
 928 of a factor of 2 in (a) and (b), and a factor of 10 and 100 in (c) and (d).

929



930

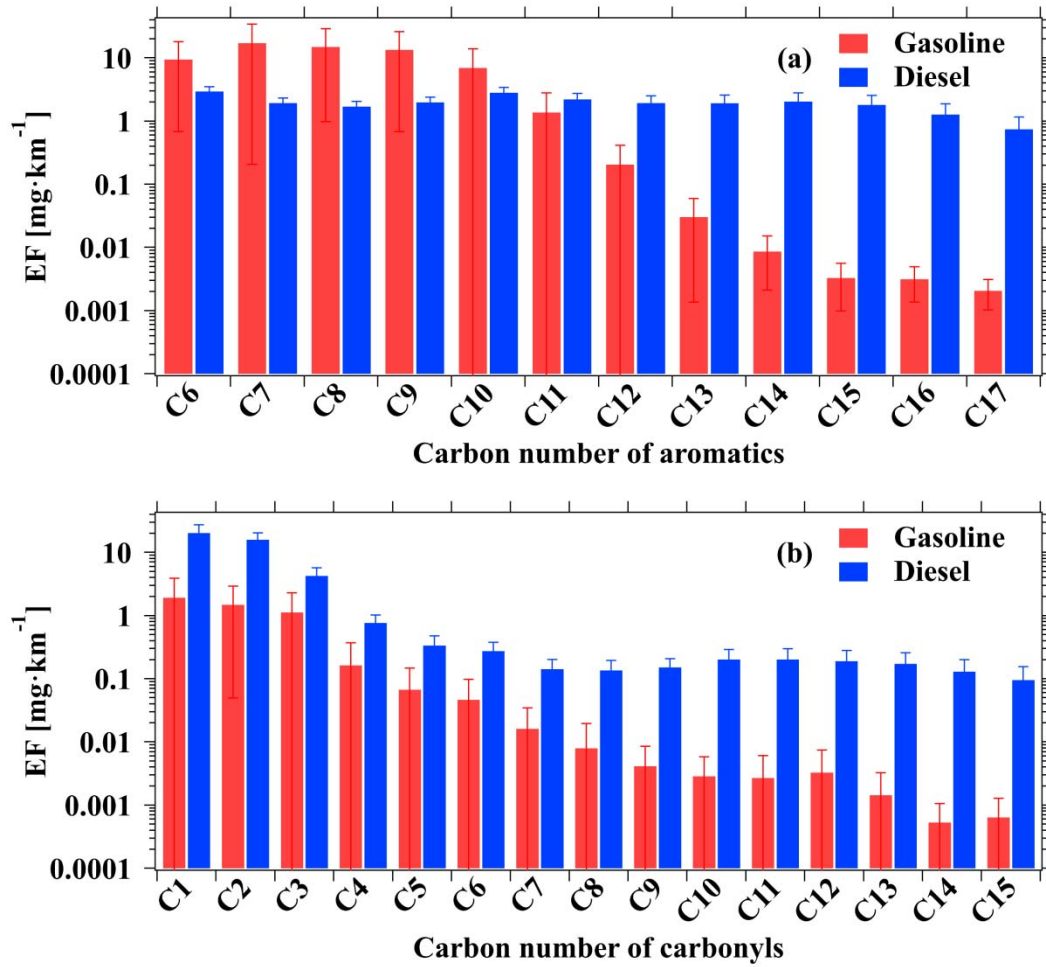
931 **Figure 8.** Scatterplot of VOCs emission factors between gasoline and diesel vehicles.

932 Each data point indicates a VOC species measured by PTR-ToF-MS. The blue line is

933 the fitted result for all data points. The black line represents 1:1 ratio, and the shaded

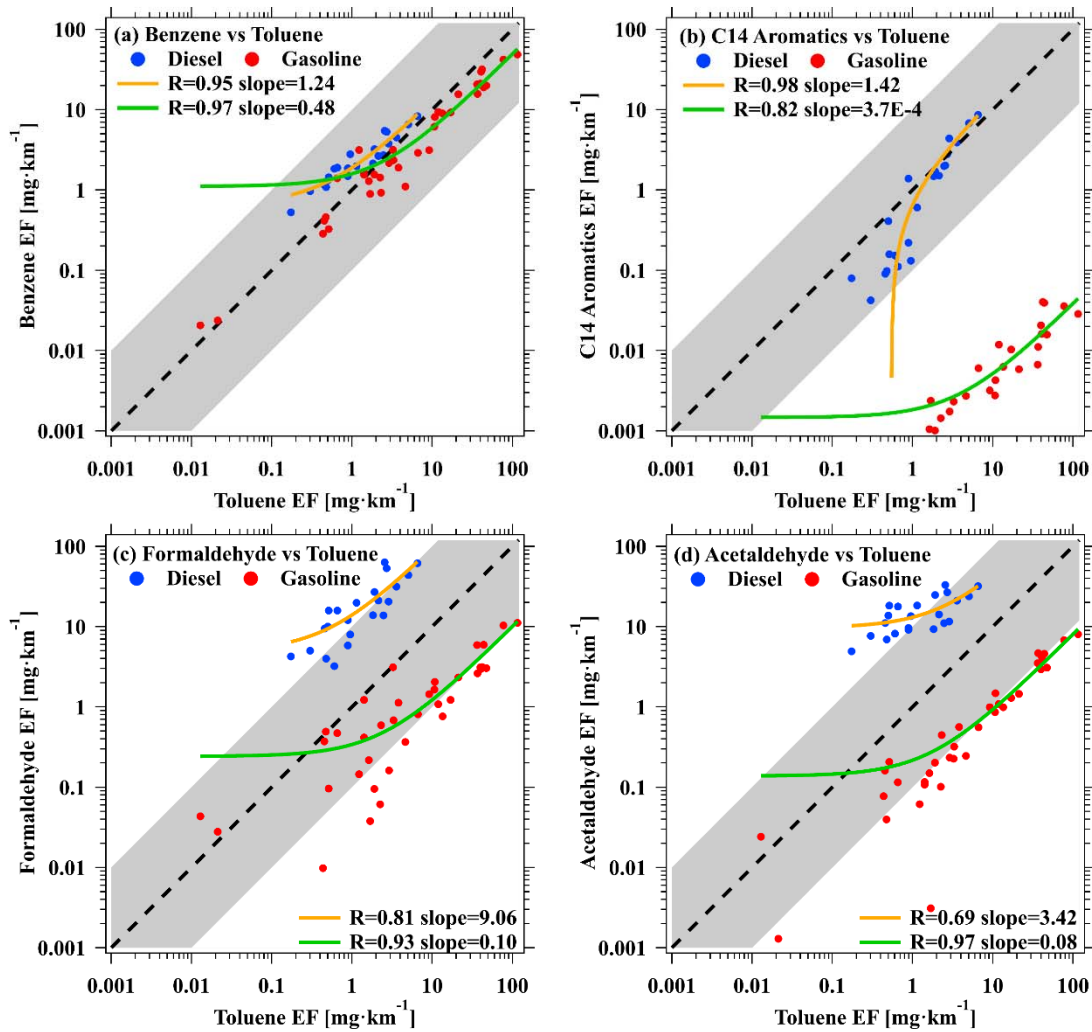
934 areas represent ratios of a factor of 10 and 100.

935



936
 937
 938
 939
 940

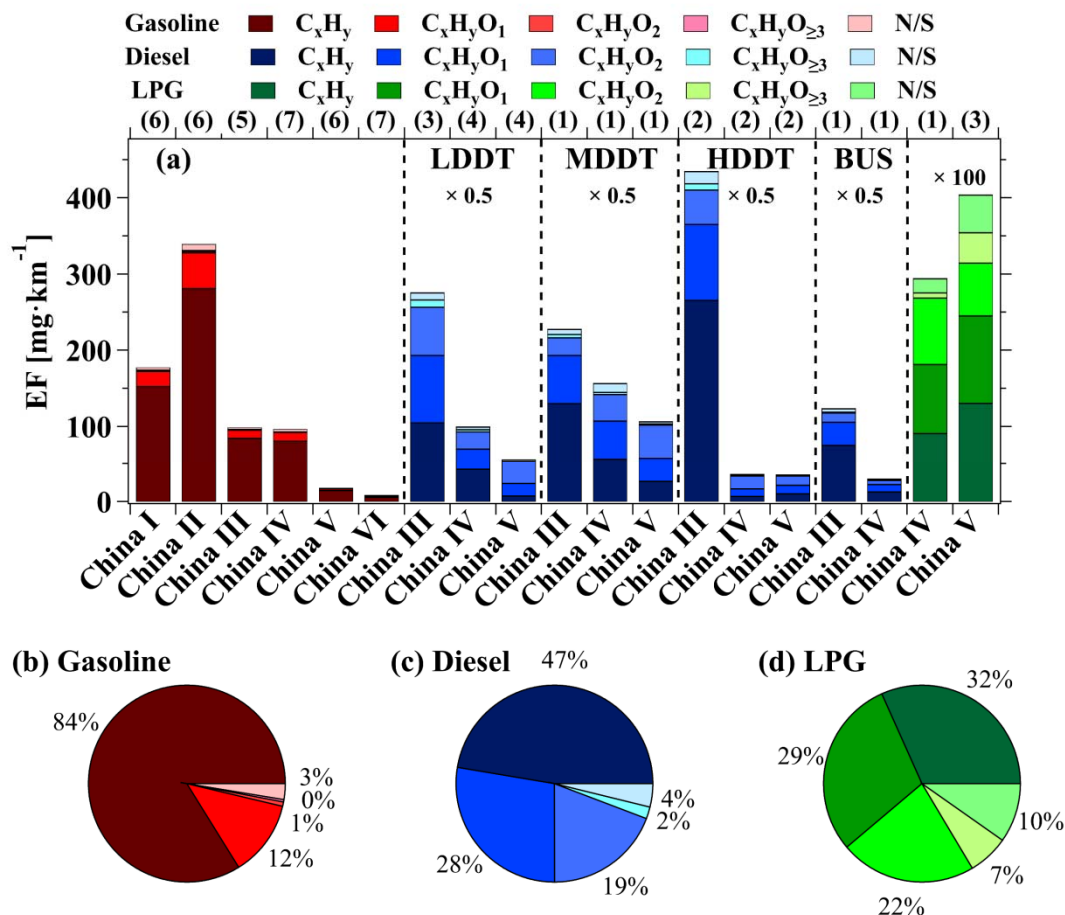
Figure 9. The determined emission factors of (a) aromatics and (b) carbonyls for each carbon number from gasoline and diesel vehicles. Error bars represent standard deviations of the emission factors for the VOCs of different carbon number.



941

942 **Figure 10.** Scatterplots of the determined mileage-based emission factors of (a)
 943 benzene versus toluene, (b) C₁₄ aromatics versus toluene, (c) formaldehyde versus
 944 toluene, and (d) acetaldehyde versus toluene for gasoline and diesel vehicles. Each data
 945 point represents each test vehicle in this study. The green and orange lines are the fitted
 946 results for gasoline and diesel vehicle. The black line represents 1:1 ratio, and the
 947 shaded areas represent ratio of a factor of 10. The green and orange line are the fits to
 948 gasoline and diesel points in each plot. Note that these linear fits are shown in curves
 949 in log-log space as the result of non-zero y-intercept.

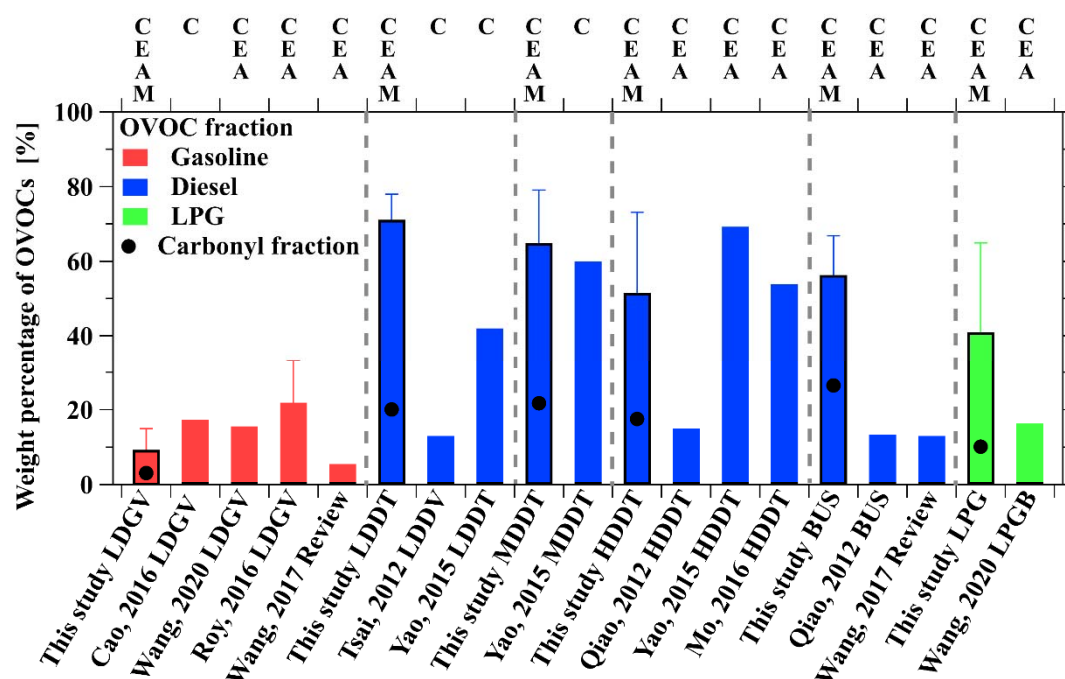
950



951

952 **Figure 11.** (a) The determined average emission factors for different emission standard
 953 from gasoline, diesel (×0.5), and LPG (×100) vehicles measured by PTR-ToF-MS. The
 954 different ion categories are discussed in the manuscript. Fractions of the determined
 955 average emission factors of VOCs ions in different ion categories from (b) gasoline, (c)
 956 diesel, and (d) LPG vehicles. The numbers above the top axis represent the number of
 957 all experiments (including multiple measurements for individual test vehicle) for each
 958 emission standard.

959



961

962 **Figure 12.** Comparison of OVOCs fractions determined in this study and those in
 963 previous studies. Error bars represent the standard deviations of the weight percentage
 964 of OVOCs. The C, E, A, M above the top axis represent the four groups of OVOCs
 965 measured in this study or previous studies, including Carbonyl: C, Ester/Ether: E,
 966 Alcohol: A, Multiple-functional: M.